Energy Science

Master Thesis

TECHNICAL AND ECONOMIC EVALUATION OF DIFFERENT UTILIZATION OPTIONS BASED ON COMBINED PHOTOVOLTAIC AND SOLAR THERMAL (PVT) SYSTEMS FOR THE RESIDENTIAL SECTOR

Name:	Luuk Veeken
Student number:	3373355
E-mail:	l.p.veeken@uu.nl
Supervisor:	Martin Ruiter (QING Sustainable)
First reader	dr. Evert Nieuwlaar (Utrecht University)
Second reader:	dr. Wilfried van Sark (Utrecht University)

Date:	01/27/2014 – 07/25/2014
Study load:	30 ECTS

QING sustainable

Universiteit Utrecht

This research is performed within the Nanosol project

Abstract:

In this report glazed and unglazed channel tubed PVT collectors are examined and research is conducted to find the most suitable heat application for different household sizes. Also a prototype unglazed channel tubed PVT collector developed within the Nanosol project is experimentally tested and these results have been used to validate the simulation model. The simulations make use of a 1 dimensional thermal model based on the equations of Hottel and Whillier. The glazed and unglazed PVT collectors are optimised for different PV types, tubing materials, dimensions, flow rate and other parameters. The objective of the optimisation procedure is to find the lowest payback period and the highest exergy production. Earlier research has pointed out that the three most promising heat applications for PVT collectors are preheating DHW, preheating water for a heat pump to provide low temperature central heating and a combination of both. The total system makes use of the optimised PVT collectors and this system is optimised for different sizes and capacities of the system components and different control schemes for the operation of the circulation pump. The optimisation is based on reducing the simple payback period. Results show that the lowest simple payback period is for using an unglazed PVT collector applied for preheating DHW for a large household. The optimised simple payback period for this PVT system is 8.4 years and mainly the electric yield is decisive for this result. This optimised system has a collector area of 34.4 m^2 and a storage tank volume of 216 L. Another observation is that a small flow rate is often optimal since this leads to higher PVT outlet temperatures resulting in a higher operation time of the circulation pump. Aside from the associated gas savings, a higher operation time also results in more cooling which increases the electrical yield of the PV cells. Using PVT collectors for preheating water in a heat pump is less beneficial and the lowest payback period is achieved by a glazed PVT collector (16.4 years). A combination of both systems led to comparable results to the PVT heat pump system. Still the additional functionality enabling the system to preheat water for DHW reduced the simple payback period slightly to 15.8 years.

Table of contents

Nomenclature

A	surface area, m^2
C_p	specific heat, J/kg K
c	thermal conductance, W/(m K)
D	diameter of water tube, m
E	electric power generated, W
G	solar radiation intensity, W/m^2
g	gravity, m/s^2
H	heat power generated, W
HX	heat exchanger
h	heat transfer coefficient $W/(m^2 K)$
k	thermal conductivity, W/(m K)
L	length, m
M	mass, kg
$\dot{m}$	mass flow rate, kg/s
N	number of water tubes; nodes in storage tank
Nu	nusselt number, -
Pr	prandtl number, -
p	perimeter
Q	energy flux, W
R	thermal resistance, K/W
Re	reynolds number, -
S	absorbed solar energy, W/m^2
T	temperature, K
t	time, s
W	width or spacing, m
r	radiation
x	distance, m
U	heat loss coefficient, W/m^2
V	velocity (m/s)
UA	loss coefficient-area product, W/K
u	speed
Greek	
α	Thermal diffusivity, m^2/s
β	Volumetric coefficient of expansion, 1/K; temperature coefficient, -
δ	thickness or depth, m
ε	emissivity, -
η	efficiency, -
Φ	collector tilt, º
σ	Stefan-Boltzman constant, $W/(m^2 K^4)$
$(\tau\alpha)_{eff}$	effective transmittance absorptance product, -
ν	kinematic viscosity
Subscripts	
ad	adhesive layer
a	ambient
air	air
b	absorber plate; back
bo	bond
c	convective
cell	solar cell
e	environment; electrical; edge
g	glass cover
gr	ground
i	inner; insulation material; inlet
l	loss, liquid
lam	PV laminate
m	mean
nom	nominal
o	outer; outlet
p	pv plate
pvt	total pvt collector
s	sky; storage
ref	reference
t	top; tube
ther	thermal
u	usefull; surrounding
w	wind; water

1 Introduction

1.1 Background

Some of the major challenges that the modern society faces are related to energy. These issues include the security of supply of fossil resources, a growing demand for energy and the associated CO_2 emissions that contribute substantially to climate change (IPCC, 2007).

In 2009, the residential sector accounted for around 19 % of the total final energy demand in the Netherlands. Of this total final energy demand 68 % is used as electricity and the remainder as heat (IEA, 2013). At this moment the largest share of this energy comes from fossil energy carriers. It is however expected that this will change as the Dutch government has set a target stating that 14 % of the gross final energy consumption has to be covered by renewables in 2020 (SER, 2013).

The residential sector could potentially play a significant role in achieving this target by investing in sustainable energy production options. Possible technologies that are already used in this sector are the generation of electricity by photovoltaics (PV) and the generation of heat by solar thermal collectors. Still in 2012 these technologies only represented a share of 0.07 % of the final electricity consumption and a share of 0.03 % of the final heat consumption respectively in the Netherlands (CBS, 2013). It is however believed that decreasing installation costs, increasing system efficiencies and increasing awareness surrounding sustainability will lead to higher adoption rates.

Since the available roof space of households is confined, a combination of PV with solar thermal systems could potentially result in higher energy yields per square meter. This combination is called photovoltaic thermal hybrid solar collector (PVT) and produces electricity and heat simultaneously. Another advantage of this system is that only one building element is required to produce both forms of solar energy. It is therefore expected that the application of PVT will lead to reductions in system balancing costs and installation costs as compared to the separate systems (ECN, 2005).

In the last 35 years a significant amount of research on the PVT technology has been conducted. Nevertheless, this has not yet led to a commercial breakthrough, as there are only a limited amount of commercial PVT applications available on the market today (Chow T. , 2010). The main reasons for this can be attributed to the tradeoff between electrical and thermal efficiency, the uncertain product reliability and high costs of the solar panel (ECN, 2005). Still there are some examples of commercial available PVT collectors such as TripleSolar BV that produces unglazed PVT collectors on the Dutch market.

1.2 Nanosol project

The Nanosol project, initiated by DNV GL, QING groep, Hyet Solar, MS Innotech and Nano Analytics, aims at developing and commercializing the PVT technology. In the PVT system a flexible thin-film amorphous silicon PV module developed by Hyet Solar will be used as the PV part of the system. This PV module is still being developed and it is expected that this module will be market ready at the end of 2014. Within the Nanosol project theoretical and experimental research is conducted to obtain the optimal design parameters for the PVT system. These parameters include the medium for heat extraction, the sizes of the different components present in the system and many others.

The partners within the Nanosol project have decided to investigate the commercialization options for the commercial and the public services sector and for the residential sector. It is however expected that the market for PVT will show similarities with the market for solar thermal collectors, which implies that the largest market potential (around 90%) will lie in the residential sector (ECN, 2005) (Chow T. , 2010). The following reasons have been given to support this claim:

- Households tolerate longer payback periods
- Energy savings obtained by households result in higher financial savings due to a higher energy price
- Inhabitants are more often environmentally or socially motivated

A large determinant of the success of a PVT system is the way in which heat is utilized. Another objective within the Nanosol project is therefore to explore different options for utilizing the produced heat of a PVT system. Since the PVT heat production is weather dependent, and therefore intermittent, it is difficult to equate supply and demand. This given has huge consequences for the optimal design of the PVT system and the different options for heat utilization as will be explained in later chapters.

1.3 Master thesis

This thesis shall be complementary to the research within the Nanosol project and is aimed at the identification and evaluation of appropriate heat utilization options for PVT. This includes a technical and economic evaluation of a selection of different promising options and a comparison with a reference case. All these evaluations will be modeled in a way that different design considerations are parameterized. This will enable the model to determine the most optimal choice of design. Additionally the model will be based on realistic environmental and external conditions by using weather and energy demand data as input. This will result in a realistic approximation of the annual yield of the combined system and will provide information on which option is optimal in economic terms and how this relates to a reference case. Next to this a prototype is developed and tested by DNV GL. This experimental data shall be used to validate the model.

The main research question of this master thesis is:

"What is the most cost effective design of a PVT and heat utilization system applied in residential sector in the Netherlands?"

Additional research questions are formulated below:

- What are energy demand patterns for heating and hot water use of different representative household profiles in the Netherlands?
- What are different promising heat utilization options for a PVT system applied in the residential sector in the Netherlands?
- What are the different design considerations in a PVT system influencing the heat production and the outlet temperature of the heat extraction medium?
- What are important tradeoffs in the design of a PVT and heat utilization system?
- What is the economic performance of the different optimized PVT and heat utilization systems and how does this relate to a reference case?

2 Theoretical background

This section contains important background information that is required for the understanding of the different concepts treated in this research. The principles of PVT systems, important design considerations and differences between PVT systems and conventional systems will be discussed.

2.1 Principles of PVT systems

As stated in the introduction a PVT system combines the function of a PV module and a flat plate solar thermal collector. Figure 1 shows a possible design for such a system that uses water as heat extraction medium.

Figure 1 Possible design of a PVT system (Zondag H. , de Vries, van Helden, van Zolingen, & van Steenhoven, 2002)

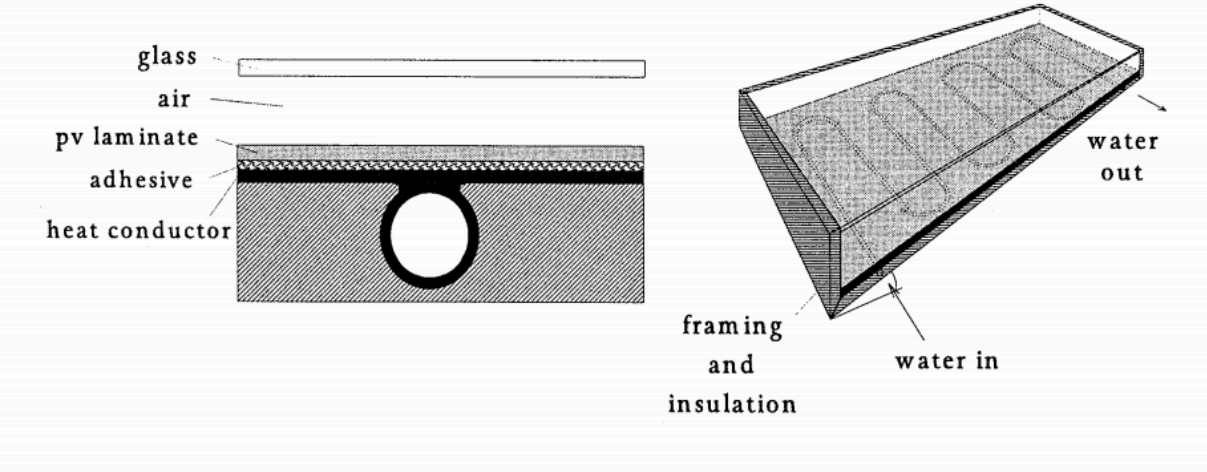

All flat plate solar thermal collectors possess an absorbing surface where solar radiation is absorbed and the associated energy is transferred to a heat extraction medium that exists in almost all cases of air or water (Twidell & Weir, 2006). In a PVT system the silicon PV module converts the energy of photons with a particular energy corresponding with the band gap of silicon into electricity. Photons that reach the surface of the PV module and do not have relevant wavelengths to generate electron-hole pairs are converted to heat and in this way the surface act as an absorber comparable with a flat-plate solar thermal collector (Chow T. , 2010). Often this PV module is attached with an adhesive to an absorber plate (heat conductor in Figure 1), which is primarily needed to transport the absorbed heat to the heat extraction medium in the tubes. Furthermore the absorber plate is fully insulated to reduce heat losses to the environment and the glass layer is opaque trapping the infrared radiation coming from the PV module. Since higher temperatures result in lower efficiencies for silicon PV modules, an extra advantage of this system compared to normal PV modules is that electrical efficiencies are higher due to the deportation of heat (Assoa, Menezo, Yezou, Fraisse, & Lefebvre, 2005).

2.2 Design considerations of PVT systems

Many different designs for flat plate PVT are developed in the last 3 decades and can be classified in many ways (Zondag H. , 2008). The most obvious classification of PVT systems would be the type of heat extraction medium, air or water. However research points out that water-based PVT collectors are more economic promising due to higher thermal performances, a greater applicability in the domestic sector and less power consumption for pumping (Zondag & van Helden, 2003). This is the reason that this report will only focus on water-based PVT collectors.

2.2.1. Water-based PVT systems

A lot of research has been done to different designs of water-based PVT systems (Charalambous, Maidment , Kalogirou, & Yiakoumetti , 2007). These systems are distinguished from each other by differing piping systems (sheet and tube or channels), amount of absorbers and amount of glass covers. In

Figure 2 four different water-based PVT groups are presented. Fig 2a shows a sheet-and-tube PVT collector where a PV module is integrated into a thermal collector and the tubes are all at a certain distance from each other. In Fig 2b a channel PVT collector with the channel above the PV module (can also be constructed under the module) is shown. This channel exists of rectangular water tubes attached to each other. Fig 2c demonstrates a design where unrestrained water flows over the absorber without a glass layer separating the air layer from the water. In Fig 2d a PVT collector with two absorbers is pictured. Transparent PV laminate act as the primary absorber and a black metal plate as the secondary absorber.

Figure 2 Different groups of water-based PVT systems (H.A. Zondag, de Vries, van Helden, van Zolingen, & van Steenhoven, 2003)

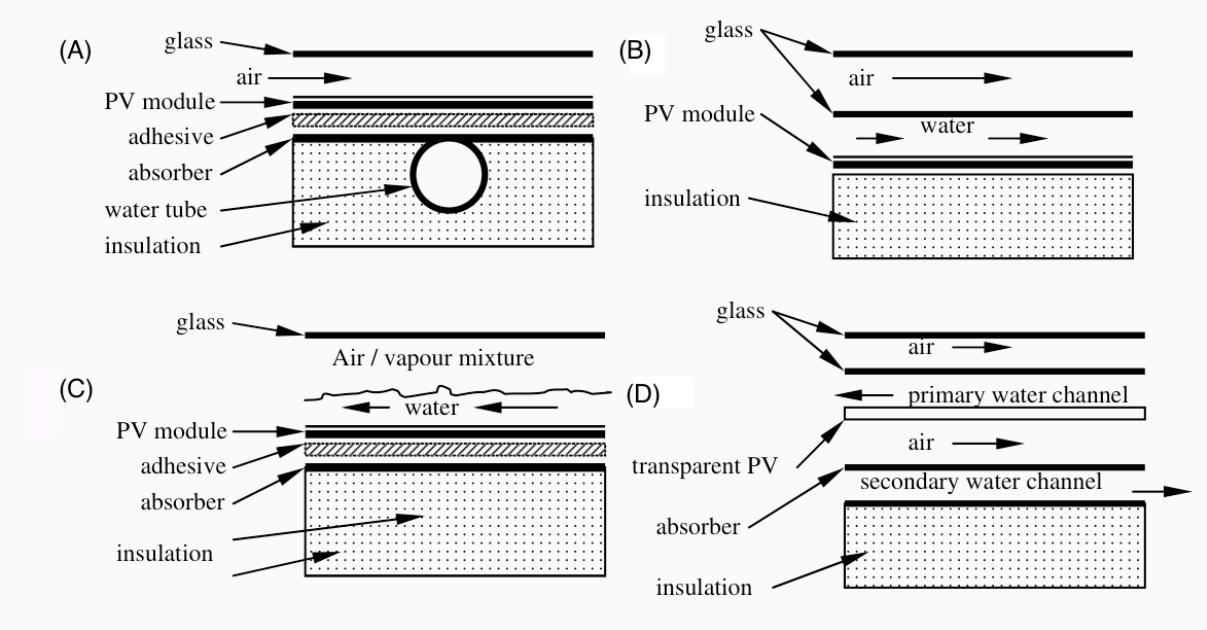

These groups can be further specified in subcategories, which are shown in Table 1. In Table 1 the annual thermal efficiencies are given for a system where the PVT collector is coupled to a storage tank and auxiliary boiler to function as preheater for domestic hot water (DHW).

Table 1 Average annual efficiencies for different types of water-based PVT collectors (Zondag H. , de Vries, van Helden, van Zolingen, & van Steenhoven, 2003)

Group	Subcategory	Annual thermal efficiency	Annual electrical efficiency
PV	-	-	0.072
(a) Sheet and tube	Unglazed	0.24	0.076
Sheet and tube	1 cover	0.35	0.066
Sheet and tube	2 covers	0.38	0.058
(b) Channel PVT	Above PV	0.38	0.061
Channel PVT	Below opaque PV	0.35	0.067
Channel PVT	Below transparent PV	0.37	0.065
(c) Free flow PVT	-	0.34	0.063
(d) Two-absorber PVT	Insulated type	0.39	0.061
Two-absorber PVT	Non-insulated type	0.37	0.061
Thermal collector	-	0.51	-

It becomes clear that a trade-off exists between obtaining a high electrical efficiency and thermal efficiency. This is mainly the result of the presence of additional insulation layers (like a glass cover or water channels above the PV), which increase the thermal efficiency by minimizing heat losses but, on the other hand, decrease electrical efficiencies due to additional reflection and higher cell temperatures.

2.3 Comparison between PVT systems and separated solar thermal collectors and PV

Since PVT collectors are a combination of solar thermal collectors and PV panels they share a lot of the same features. Still there are some important differences between the combined and separated system and those differences can play a major role in the final design of a PVT collector. In this section PVT systems are compared with flat plate solar thermal collectors and PV panels individually.

2.3.1. PVT system and solar thermal collector

The thermal efficiency of a PVT or solar thermal collector is often presented using efficiency curves as a function of reduced temperature ($\frac{(T_{in}-T_a)}{G}$), where T_a (ambient temperature), G (solar radiation) and V_w (wind speed) are kept constant at certain conditions and T_{in} (inlet temperature) becomes larger (Duffie & Beckman, 2013). This method is standardized and globally acknowledged as main procedure for determining the performance of solar thermal collectors and is therefore also commonly used to evaluate the thermal performance of a PVT collector (Zondag H. , 2008). In Figure 3 the efficiency curves are presented for a conventional solar

thermal collector, an unglazed sheet and tube PVT collector and a sheet and tube PVT collector with a glass cover.

Figure 3 Efficiency curves of a thermal collector and two types of PVT collectors (Zondag H. , 2008)

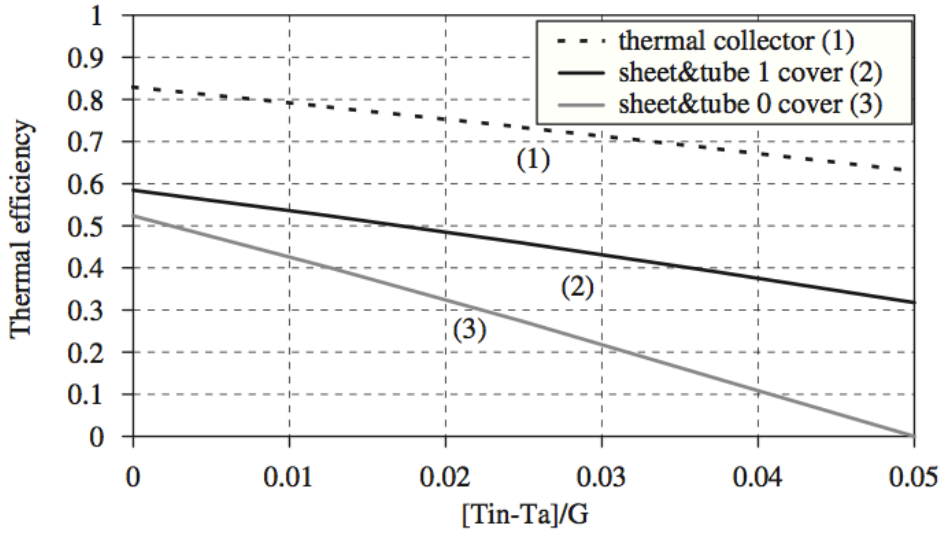

Figure 3 shows large deviations between a conventional collector and PVT collectors, this is due to a variety of reasons that are summarized below (Huang, Lin, Hung , & Sun, 2001):

- In a PVT system a portion of the incoming radiation is converted into electrical energy resulting in less available energy for heat purposes
- The absorption factor of a PV-surface is lower than that of a flat plate collector absorber since various layers in the PV-laminate reflect some of the incoming radiation
- The surface of a flat plate collector is spectrally selective resulting in less thermal radiation losses than a PVT collector
- In a PVT collector the PV has to be connected to a piping system (tubes or channels) indicating that additional materials are required. Also the PV exists of multiple materials which main function is not to conduct heat. These reasons result in the fact that the heat resistance in PVT collectors is higher which leads to a relatively hot PV surface and additional heat losses

A lower thermal efficiency will also result in lower collector outlet temperatures at equal flow rates and thus potentially differing applications.

2.3.2. PVT system and PV

The type of PV panel that is used in the system is the main determinant of the electrical efficiency of a PVT collector. In literature mainly amorphous silicon (a-Si) and crystalline silicon (c-Si) PV panels are investigated and aside from different electrical efficiencies the type of PV panel will also influence the thermal efficiency as explained in the previous section by influencing absorption and emissivity

(Zondag H. , 2008). The following characteristics of PVT collectors will influence the discrepancy of electrical efficiencies between PVT and conventional PV (Charalambous, Maidment , Kalogirou, & Yiakoumetti , 2007):

- The efficiency of PV panels decrease with increasing cell temperature. Some types of PV, like c-Si PV, are more sensitive to temperature changes than others. In the case of PVT collector, a well-insulated system will reach higher cell temperatures and this will result in lower electrical efficiencies. On the other hand a PVT system that isn't well insulated like an unglazed collector can be more efficient than conventional PV due to potential cooling effects by convection and extraction of heat by the circulating fluid
- The presence of additional layers such as a cover or a water channel lead to less transmission of solar radiation in PVT systems than conventional PV which will decrease the electrical efficiency

Both effects can be observed in Table 1, where an unglazed sheet and tube collector reaches a higher efficiency than normal PV and a two-cover collector a significantly lower one due to higher temperatures (well-insulated) and lower transmission. Note that the flow rate of the water circulated through the PVT system has an influence on both the thermal and electrical efficiency:

- A low flow rate will result in higher temperatures and thus more thermal losses and a lower electrical efficiency due to higher cell temperatures
- A high flow rate will result in lower temperatures and higher electrical and thermal efficiencies. Still there is a tradeoff since low temperature water has less value and higher flow rates will result in higher pump power consumptions.

2.4 Manufacturing aspects of PVT systems

The simplest way to build a PVT collector is by glueing a PV cell or entire laminate to the absorber of a thermal collector. This manufacturing technique is applied in many experimental research projects (Zondag H. , 2008). One disadvantage of glueing solely PV cells to a thermal collector is that potentially the PV will not be sufficiently protected against moisture. Also problems could occur due to poor electrical insulation, as the thermal collectors are often copper-based. These problems can be avoided by using commercial PV laminate, however this will result in certain drawbacks as well (Zondag H. , 2008):

- Increases the thermal resistance between the PV and the absorber due to extra layers such as Ethylene/Vinyl Acetate (EVA) or tedlar
- Results in an additional glueing step leading to higher manufacturing costs

It is also possible to laminate the whole PV laminate to the absorber and this technique is especially preferred if the lamination step could be executed without using high temperatures since this could lead to bending of the PVT laminate due to different thermal expansion coefficients of the materials.

To maintain low costs researchers have also experimented with other types of absorber material instead of the more common copper thermal collectors (Sandnes & Rekstad, 2002). It is shown that glazed PVT systems could be build with polymer thermal collectors as absorber where an elastic silicon adhesive had to be used to compensate for higher thermal expansions coefficients accompanying polymers.

For the commercial application of PVT systems reliability, despite very limited attention in literature, is a very important topic (Zondag H. , 2008). Major aspects that are believed to play an important role in the reliability of the system are summarized below:

- Stagnation temperature

Especially glazed PVT collectors can establish high temperatures when the storage tank is already maximal filled with heat. These temperatures can rise up to 130 ºC exceeding stagnation temperatures of normal PV laminates (Zondag & Van Helden, 2002). This can lead to deterioration of the top film or encapsulation material.

- Thermal shocks

Rapid temperature changes due to a specific operation of the control scheme of the circulation pump could potentially be harmful for the lifetime of a PVT system. Due to different thermal expansions coefficients materials could potentially wear off.

- Ambient conditions

Changing ambient conditions can result in high humidity, ice formation, hailstones, and other weather dependent consequences that could impact especially the exterior of the PVT system. It is therefore important that materials such as the glass cover and adhesive are chosen not only to serve energy efficiency objectives but also provide sufficient stability and durability.

2.5 Heat utilization options for PVT systems

As mentioned before the design type and operation conditions have a large influence on the temperature range of the extracted fluid. Also the influence of which heat efficiency loss mechanism is dominant is highly dependent on the operating conditions. Next to this, the production of thermal energy by a PVT collector is often not coupled to thermal energy demand; in fact, often the opposite is true. Additionally the sizing of the different components present in a complete PVT system with a heat utilizing capability will play a large role as well (Santbergen, Rindt, Zondag, & van Zolingen, 2010). To summarize it is more meaningful to calculate the efficiency of the whole system, than for an individual PVT collector. Additionally since weather conditions vary on a daily and seasonal basis it is important to aim at high annual yields.

An important aspect in determining useful utilizing heat options for PVT systems is the temperature range of the extracted water. For glazed collectors this is typically around 30-60 ºC and for unglazed 20-50 ºC. Note that these numbers are

dependent on the type of PVT collector, design considerations, operation conditions, presence of a storage tank and the control scheme of the circulation pump. In Figure 4 the efficiency curves are presented for different conventional solar thermal collectors. Also the application of the utilized heat is presented as a range and this graph shows that this is very dependent on the temperature of the extracted water.

Figure 4 Efficiency curve for conventional solar thermal collectors (Kalogirou, 2004)

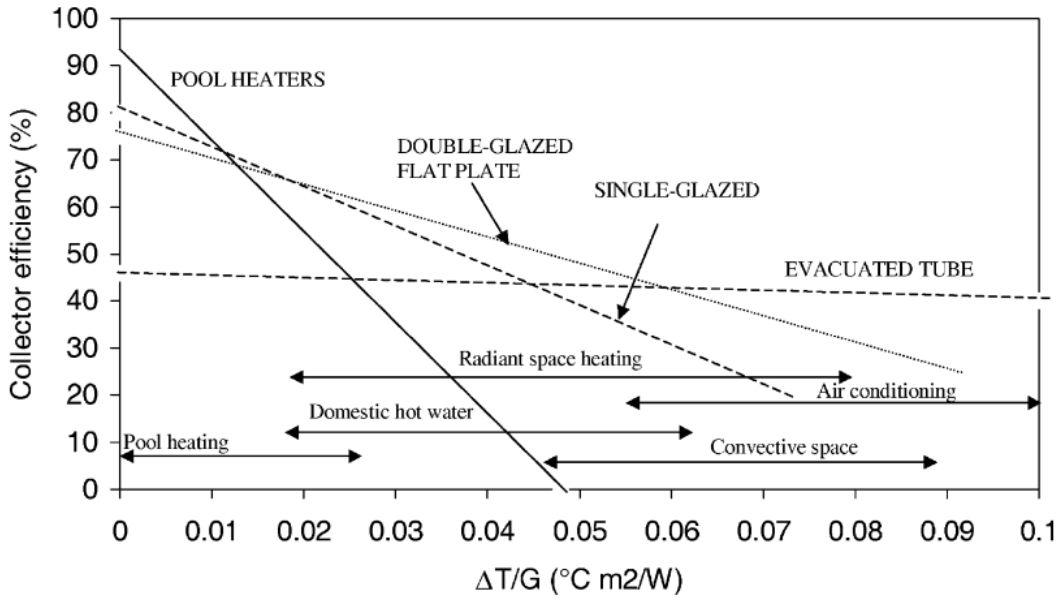

A lot of researchers have looked for promising heat utilization options for PVT collectors and a large amount of systems are examined. The most common application for PVT collectors that is examined is for preheating DHW, which is also the most common application for conventional solar thermal collectors (Kalogirou, 2004). Still there are few more possibilities for the utilization of heat and Table 2 gives an overview of the most commercial promising applications and accompanying advantages and disadvantages. The country where the research is done is also given since weather conditions differ significantly around the globe influencing the suitability of certain heat utilization options. Since this study aims at finding promising applications for PVT in a Dutch climate, especially studies have been selected where weather conditions were similar.

Table 2 Different heat utilization options for PVT

Application	Country	Advantages	Disadvantages	References
Preheater DHW	Hong Kong Netherlands	- Easy to integrate into existing infrastructure such as a boiler - Demand for DHW is relatively steady throughout the year (not much seasonal variation) - There is a lot of knowhow for this application and is already commercial	- Storage tank and heat exchanger are always needed - Demand patterns are very stochastic which can negatively affect the annual yield - Preheater is needed since PVT outlet water temperatures do not	(Ji , Chow, & He, 2003) (Santbergen, Rindt, Zondag, & van Zolingen, 2010)

		available	comply with regulations	
Preheater heat pump for low temperature space heating	Netherlands	- Possibility to cover a large part of the total heating demand of a dwelling by PVT (producing electricity and heat for heat pump) - Higher electrical yields due to low water inlet temperature - Obtain a higher COP and higher heat pump operation times than in reference	- Dimensioning of the system is very difficult - Requires a huge investment and installation - Heat demand is high in winter while production is low: combination needed with auxiliary boiler and seasonal storage or geothermal reservoir	(Bakker, Zondag, Elswijk, Strootman, & Jong, 2004) (Zondag & van Helden, 2003)
Combination of above applications	Netherlands	- Results in a higher annual yield than separated heat applications - Already commercial available	- Results in higher investment costs and more complex system than separated heat applications - Dimensioning and control scheme is more difficult than separated heat applications	(Triple Solar, 2013)

2.6 Scientific background PVT

The goal of this research is to find the most cost effective design of a PVT and heat utilization system that can be applied in the Netherlands. A simulation model has been developed which is able to simulate different PVT systems coupled to different heat utilization systems. Since not all options could be evaluated due to time constraints, a selection had to be made and this is done based on the most economic promising PVT and heat utilization for a Dutch climate as shown in Table 2. Before explaining the modeling methodology it is important to give some scientific background concerning the PVT collector, as this will form the backbone of the simulation model.

2.6.1 Accuracy and computation time of different models

A detailed analysis of a flat plate solar thermal collector is a complicated problem due to the complexity of temperature distributions in three dimensions. Hottel and Whillier therefore derived some basic equations that resulted in a relatively simple one-dimensional analysis with very useful results, especially for long-term evaluations of solar thermal collectors (Hottel & Whillier, 1958). In the textbook 'Solar Engineering of Thermal Processes' these equations are explained and many researchers use these equations, adjust them to PVT collectors and generate a steady-state model that can evaluate on a wide variety of time scales (Duffie & Beckman, 1991) (Chow T. , 2010). Another reason to use this more simple one-dimensional analysis is that the computation time is very short when compared with more complex two-dimensional or three-dimensional models. It is stated that one-dimensional models are most suitable for annual calculations since they show a

combination of good accuracy and limited computation time (Table 3) (Zondag H. , de Vries, van Helden, van Zolingen, & van Steenhoven, 2002).

Table 3 Advantages and computation time of four different models

Model type	Characteristics	Calculation time	
		Efficiency curve computing time	Hourly computing time
1D steady model	Fast calculation of daily and annually averaged yield for sheet-and-tube design	0.27 s	0.05 s
2D steady model	Like 1D steady model but easily adapted to other configurations	8.35 s	1.67 s
3D steady model	Like 2D steady model but also detailed information on temperature distribution	229.31 s	45.86 s
3D dynamic model	Like 3D steady model but also calculation of instantaneous yield for non-steady conditions	-	2.5 h

2.6.2 Explanation and equations of the steady-state 1D model

In this section it is explained how a 1D model is generated and how equations, as derived by Hottel, Whillier, Duffie and Beckman, are adjusted to function in a PVT simulation model. These equations are based on a flat plate solar thermal collector with a cover and a sheet and tube design. Where stated adjustments have been made for unglazed and channel collectors.

As solar radiation is transmitted through the cover, it is absorbed by the PV surface and energy is transferred to the tubes and extracted by the fluid. As shown in Fig 5a and c, the tube region has a lower temperature since the liquid extracts heat from the surface. In the Y direction (Fig 5b and d), the temperature distribution is increasing because the liquid is heated.

Figure 5 Temperature distribution on an absorber plate (Duffie & Beckman, 2013)

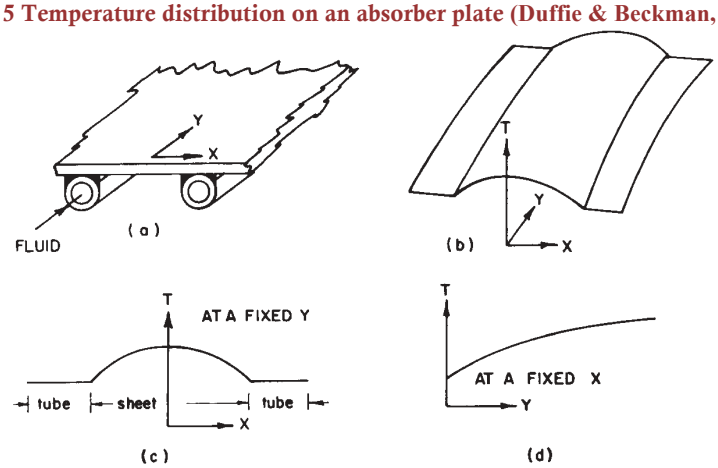

To simulate the situation as showed in Figure 5 a number of assumptions had to be made which are described below (Duffie & Beckman, 1991):

1. Performance is steady state.
2. The headers cover a small area of collector and can be neglected.
3. The headers provide uniform flow to tubes.
4. Heat flow through a cover is one-dimensional.
5. There is a negligible temperature drop through a cover.
6. The covers are opaque to infrared radiation.
7. There is one-dimensional heat flow through back insulation.
8. The sky can be considered as a blackbody for long-wavelength radiation at an equivalent sky temperature.
9. Temperature gradients around tubes can be neglected.
10. The temperature gradients in the direction of flow and between the tubes can be treated independently.
11. Loss through front and back are to the same ambient temperature.
12. Dust and dirt on the collector are negligible.
13. Shading of the collector absorber plate is negligible.

In steady state the useful energy output of a collector of area A_{pvt} is the difference between the absorbed solar radiation and the thermal loss (Duffie & Beckman, 1991):

$$Q_u = A_{pvt}[G - U_l(T_{pm} - T_a)] \quad (1)$$

Q_u = useful energy
A_{pvt} = PVT collector area
G = solar radiation
U_l = overall heat loss coefficient
T_{pm} = average temperature of the PV plate
T_a= ambient temperature

In order to simplify the mathematics, it is useful to define an overall loss coefficient. In this coefficient, the heat losses consist of radiation, convection and conduction and can be represented in a thermal network as shown in Figure 6. Here it is shown that before the solar radiation enters the cover, some energy is lost by shortwave radiation losses. The PV plate will absorb the majority of the solar radiation energy, but some of this absorbed energy will be lost by radiation and convection to the

glass cover. Also the glass cover absorbs some energy from the solar energy source and this energy, including the radiation and convection gains by the PV plate, will be lost by radiation and convection to the environment. The PV converts a part of the solar radiation into electricity and the remaining energy is transferred from the PV plate to the absorber plate and the tubes. Some of this energy is then transferred to the insulation material where it is conducted to the environment, however the water circulating through the tubes absorbs most.

Figure 6 Thermal network of a PVT collector (Chow T. , 2003)

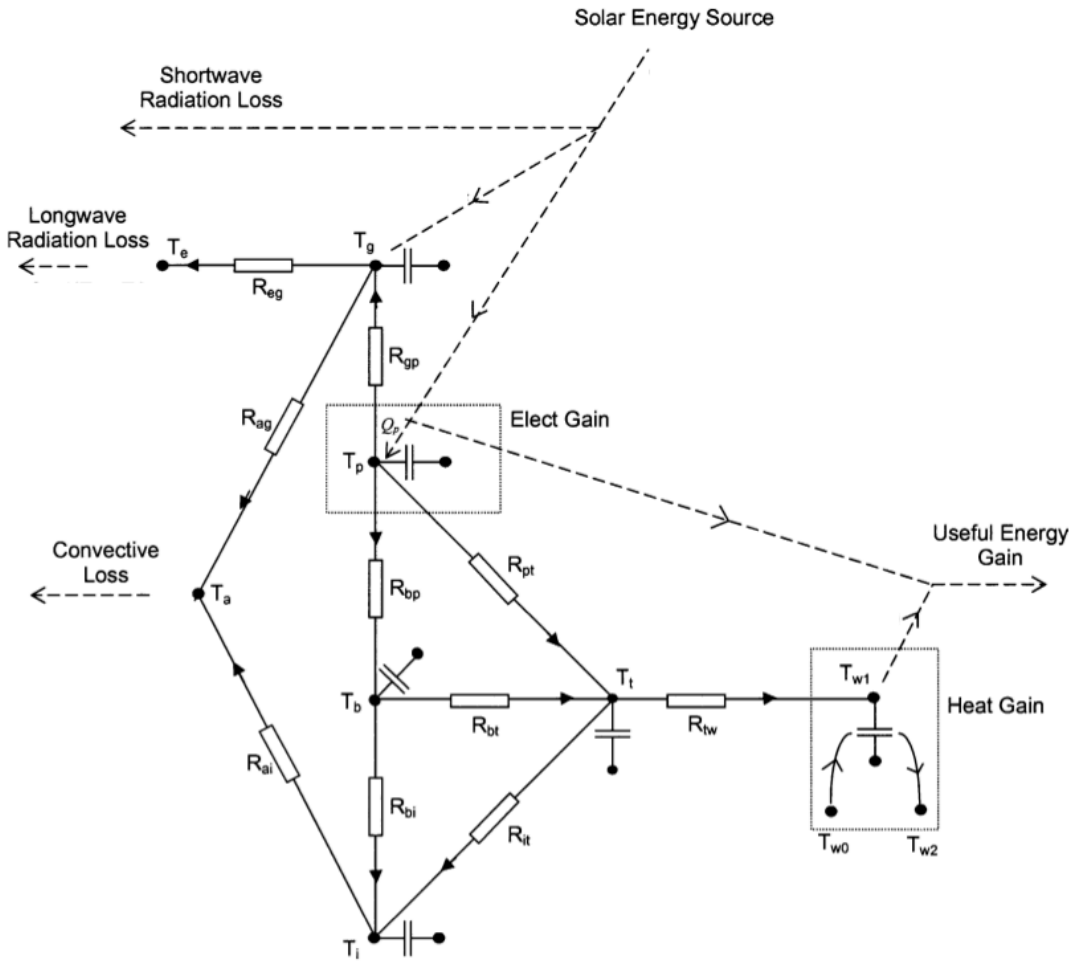

To calculate a total heat loss coefficient, first a top-loss coefficient is defined by the following equation:

$$U_t = \left(\frac{1}{h_{c,p-g} + h_{r,p-g}} + \frac{1}{h_{c,g-a} + h_{r,g-e}} \right)^{-1} \qquad (2)$$

U_t = total heat loss coefficient of the front side

$h_{c,p-g}$ = convection from the plate to the glass

$h_{r,p-g}$ = radiation from the plate to the glass

$h_{c,g-a}$ = convection from the glass to the ambient

$h_{r,g-e}$ = radiation from the glass to the environment

The radiation coefficient from the plate to the glass cover is:

$$h_{r,p-g} = \frac{\sigma(T_p^2 + T_g^2) - (T_p + T_g)}{\frac{1}{\varepsilon_p} + \frac{1}{\varepsilon_g} - 1} \quad (3)$$

T_p = temperature of the plate
T_g = temperature of the glass
ε_p = emmisitivity of the plate
ε_g = emmisitivity of the glass

The radiation coefficient from the glass cover to the ambient is:

$$h_{r,g-e} = \varepsilon_g \sigma(T_g^2 + T_s^2) - (T_g + T_s) \quad (4)$$

T_s = temperature of the sky (given by the following formula: $0.0552 * T_a^{1.5}$ (Duffie & Beckman, 2013))

The convection coefficients in equation (2) are:

$$h_{c,p-g} = Nu * \frac{k}{L_{p-g}} \quad (5)$$

Nu = Nusselt number
k = thermal conductivity of air
L_{p-g} = Plate-cover distance

$$h_{c,g-a} = 3u_w + 2.8 \quad (6)$$

u_w = wind speed

The last equation is an empirical linear relation between the wind velocity and the convection on a flat plate solar thermal collector (Chow T. , 2003). This equation takes into account both free and forced convection. The Nusselt and Rayleigh number that describe how the air layer between the PV and glass cover in a flat plate solar thermal collector behave are obtained from Duffie and Beckman (Duffie & Beckman, 1991).

$$Ra = \frac{g * \beta_w * \Delta T_{p-g} * L_{p-g}^3}{\nu_w * \alpha_w} \quad (7)$$

Ra = Rayleighs number
g = gravity
β_w = volumetric coefficient of expansion

ΔT_{p-g} = temperature difference between plate and glass

v_w = kinematic viscosity

α_w = thermal diffusivity

$$Nu = 1 + 1.44\left[1 - \frac{1708(\sin 1.8\phi)^{1.6}}{Ra * \cos\phi}\right]\left[1 - \frac{1708}{Ra * \cos\phi}\right]^{+} + \left[\left(\frac{Ra * \cos\phi}{5830}\right)^{\frac{1}{3}} - 1\right]^{+} \quad (8)$$

ϕ =collector tilt

Note that equations (3) and (5) are only used in a glazed collector design. Now to determine the overall heat loss coefficient, the conduction losses from the back and the edge have to be known. The following equation is used to determine these losses:

$$U_b = \frac{k_{b,i}}{\delta_{b,i}} \quad (9)$$

U_b =heat loss coefficient back side

$K_{b,i}$ =thermal conductivity of the insulation material (back)

$\delta_{b,i}$ =thickness of the insulation material (back)

$$U_e = \frac{\frac{k_{e,i}}{\delta_{e,i}} * p_{pvt} * \delta_{pvt}}{A_{pvt}} \quad (10)$$

U_e = heat loss coefficient of the edge

$K_{e,i}$ = thermal conductivity of the insulation material (edge)

$\delta_{e,i}$ = thickness of the insulation material (edge)

p_{pvt} = perimeter of the PVT collector

δ_{pvt} = gross thickness of the PVT collector

Combine equations (2), (9) and (10) gives the overall heat loss coefficient:

$$U_l = U_t + U_b + U_e \quad (11)$$

If we temporarily assume that the temperature gradient in the flow direction is negligible it is possible to derive a fin efficiency factor and a collector efficiency factor (derivation is omitted in this report). Those factors account for the temperature distribution in the Y direction (see Fig 5c) and the heat conduction from the PV laminate to the extracting fluid respectively:

$$F = \frac{\tanh[m(W-D)/2]}{m(W-D)/2} \tag{12}$$

D = diameter of the tubes

$$F' = \frac{1}{U_l\left[\frac{1}{U_l} + \frac{1}{h_{cell-b}} + \frac{W}{4D_i h_{t-w}} + \frac{W}{C_b}\right]} \tag{13}$$

h_{cell-b} = heat transfer from cell to bond
W = length between tubes
D_i = inner diameter of tubes
h_{t-w} = heat transfer from tubes to water

Figure 7 shows the different lengths, layers and subscripts in a PVT collector for illustration purposes. In equation 12, m is defined as:

$$m = \left(\frac{U_l}{k_{lam} * \delta_{lam} + k_b + \delta_b}\right)^{-1/2} \tag{14}$$

k_{lam} = conductivity of laminate
δ_{lam} = thickness of laminate
k_b = conductivity of bond
δ_b = thickness of bond

Figure 7 Schematic view of a sheet-and-tube PVT collector

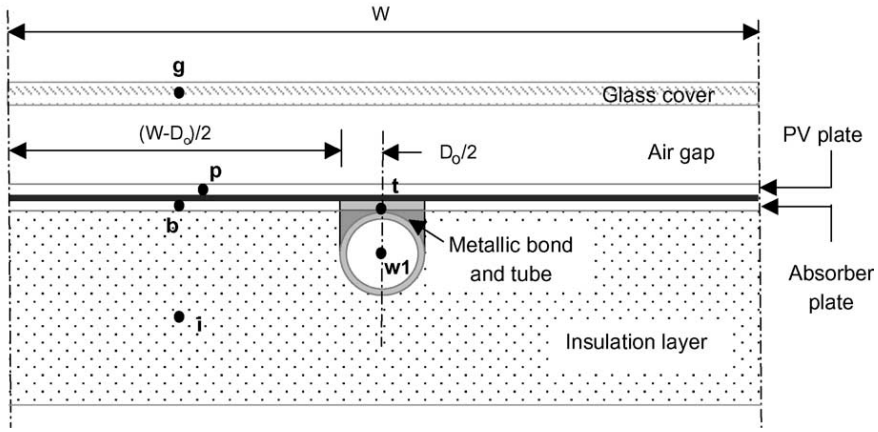

Note that in a channel design the width and diameter are equal so equation (12) becomes 1 and equation (13) becomes:

$$F' = \frac{1}{U_l\left[\frac{1}{U_l} + \frac{1}{h_{cell-b}} + \frac{D}{4D_i h_{t-w}} + \frac{D}{C_b}\right]} \tag{15}$$

In equation (13) and (15) the bond conductance (C_b) is defined as:

$$C_b = \frac{k_b * L_b}{\delta_b} \tag{16}$$

k_b = conductivity of the bond
L_b = length between bonds
δ_b = thickness of the bond

Now the temperature distribution in the flow direction has to be accounted for and this is done by defining a heat removal and a flow factor (derivation is omitted in this report):

$$F_R = \frac{\dot{m} * C_p}{A_{pvt} * U_l}\left[1 - \frac{S/U_l - (T_o - T_a)}{S/U_l - (T_i - T_a)}\right] \tag{17}$$

$\dot{m}$ = mass flow rate
C_p = heat conductivity of water (constant pressure)
S = absorbed solar energy
T_o = temperature of the outlet water
T_i = temperature of the inlet water

$$F'' = \frac{F_R}{F'} = \frac{\dot{m} * C_p}{A_{pvt} * U_l * F'}\left[1 - \exp\left(-\frac{A_{pvt} * U_l * F'}{\dot{m} * C_p}\right)\right] \tag{18}$$

This derivation is done in a way that the original equation (1) can be rewritten in terms of T_i and T_a, which are both often easily to determine:

$$Q_u = A_{pvt} * F_R[G(\tau\alpha)_{eff} - U_l(T_i - T_a)] \tag{19}$$

$(\tau\alpha)_{eff}$ = effective transmittance-absorption product

In equation (19) the effective transmittance-absorption product is integrated as well. This value accounts for the reflection of the glass cover, the absorption of the PV laminate; the effects of a higher glass cover temperature (due to absorption of sunlight) and the energy 'losses' due to electricity production by the PV. Using equation 19, the total thermal efficiency can now be expressed as function of the useful thermal energy, collector area and incoming solar radiation per square meter:

$$\eta_{ther} = \frac{Q_u}{A_{pvt} * G} \tag{20}$$

2.6.3 Electricity production of the PVT collector

It is important that the calculation of the thermal efficiency and electrical efficiency is accurate due to there interdependency. The electrical yield is calculated using an equation that is based on the following inputs:

- The reference electrical efficiency of a solar panel, which is the electrical efficiency measured at standard test conditions (25 °C ambient temperature, 1000 W/m^2 irradiance and 0.0 m/s wind speed)
- The cell temperature, which is calculated by the thermal model
- The temperature coefficient influences the loss in electrical efficiency at increasing cell temperatures. This coefficient is measured for different types of solar cells and have a significant effect on the total efficiency of the PVT system (Santbergen, Rindt, Zondag, & van Zolingen, 2010)

The following equation is used to describe the relationship between the different variables:

$$\eta_e = \eta_{e,ref}\left[1-\beta(T_{cell}-T_{a,ref})\right] \quad (21)$$

$\eta_{e,ref}$ = efficiency solar cell at standard conditions

β =temperature coefficient

T_{cell} = temperature of the PV cell

$T_{a,ref}$ = temperature at standard conditions (298.15 K)

This relationship for calculating the electrical efficiency of a solar panel is used in a large number of studies (Sarhaddi, Farahat, Ajam, Behzadmehr, & Mahdavi Adeli , 2010).

3 Methodology

In this section the methodology is explained that was used to answer the proposed research questions. A simulation model is especially developed in this thesis to accurately calculate the most optimal PVT collector and heat utilization system. First the simulation specifics are discussed. Secondly, the configuration of the different analysed PVT systems with heat application will be explained. Thirdly, the individual modelling components are dealt with. Fourthly, the methodology is discussed for modelling the loads and finally the model validation and optimization procedures will be explained.

3.1 Simulation specifics

The program developed for this study has to satisfy different requirements in order to make realistic simulations. A very important consideration is its ability to efficiently and quickly process large amounts of data since annual yields are calculated using timestamps with a period of 10 minutes (which amounts to 52560 data points each year). Another consideration is the ability to simulate on a modular basis, which indicate that different components are modelled individually and can be coupled in any desired configuration. This also means that each component has its own code and can independently operate (if it is assigned with proper material properties, physical constants, dimensioning properties and relevant input data).

TRNSYS, simulation software developed by the Solar Energy Lab, is an extremely flexible graphically based software environment used to simulate the behaviour of transient systems (TESS, 2013). This software is modular and highly efficient in processing large amounts of data, therefore many scientists use it for simulating solar thermal collectors, solar panels, PVT and many more systems (Nafey, 2005). Unfortunately this software could not be used in this thesis due to its high costs.

Another programming language that is very suitable for scientific computing is Python. This is an open-source; object oriented programming language and is more and more used for scientific purposes due to its proper functionality. Also libraries are available like NumPy and Pandas and this enables the programmer to use Python as Matlab, C++ or other programming languages. Due to these advantages and functionalities there has been chosen for Python as programming language for developing the simulation model.

3.2 System configuration

As explained in the previous chapters, the efficiency of the whole system should be considered instead of only the PVT collector since the usefulness of the produced thermal energy is very dependent on the chosen application. Since not all heat applications could be modelled, three scenarios are selected based on the most economic promising applications as the literature review pointed out (see Table 2). Still for each individual total system a number of configurations are possible as is

displayed in Figure 8. System A shows a parallel auxiliary boiler, in the configuration of system B the auxiliary boiler is in series and system C shows an additional heat exchanger to separate the water circulating through the collector with the water that is utilized by a certain load.

Figure 8 Possible system configurations (Klein, Cooper, Freeman, Beekman, Beckman, & Duffie, 1975)

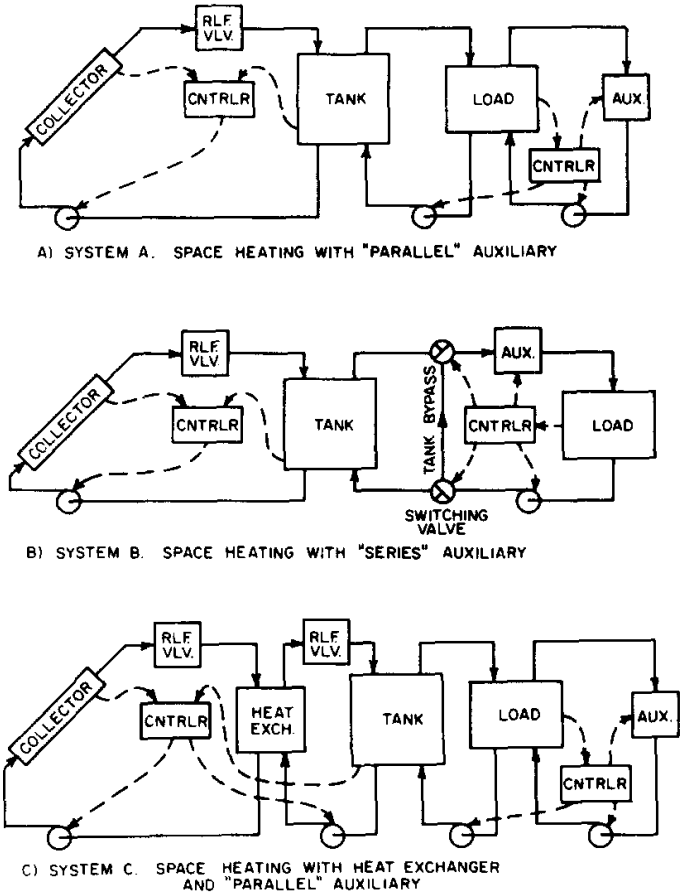

Aside from the configurations showed in Figure 8 there are many more configurations possible and this is the reason that choices have to be made since not all configurations could be evaluated due to time limitations. A basic representation of the simulated system configuration is displayed in

Figure 9. There is chosen for a heat exchanger between the circulating fluid in the first circuit (collector, pump and heat exchanger) and the second circuit (heat exchanger, storage tank, pump) because the circulating fluid contains a water/ethylene glycol mixture to protect the PVT collector against freezing events, which can occasionally occur in Dutch climate. Also a storage tank is needed for all simulated applications as described in Table 2 to function as an energy buffer between collector and application. This is required for both preheating DHW, powering a heat pump and a combination of both applications.

Figure 9 System configuration

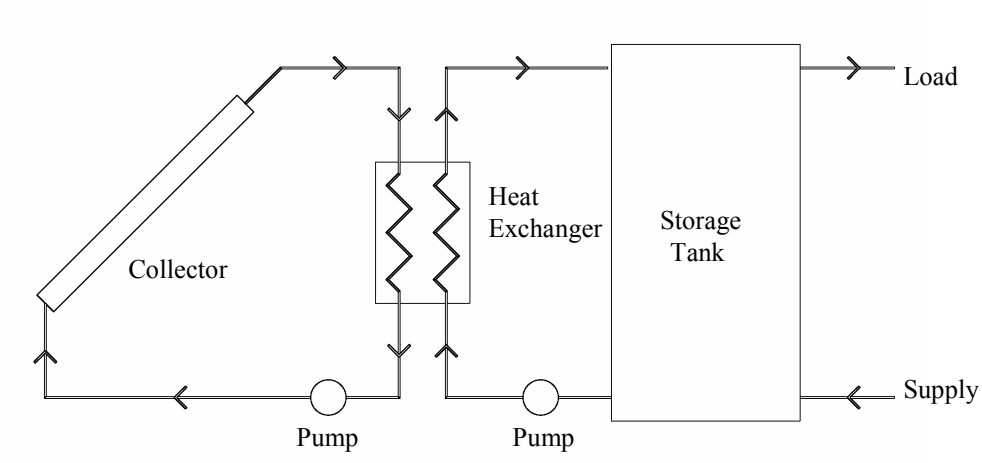

Note that the heat pump and the auxiliary boiler are left out in

Figure 9 as they both are simulated separately. The modeling of these systems and the generated load profiles functioning as input are explained in later in this chapter.

3.3 Modelling components

3.3.1 PVT

The PVT system is modeled using the adjusted Hottel and Whillier equations described in the scientific background. Just as any other simulation model it needs certain input. The first input that the simulation model uses are the system properties, which can be variable or fixed:

- Variable properties

These properties are dependent on the environment; this means that changing weather conditions like temperature, solar radiation and wind speed will influence the system properties. These properties include the thermal conductivity, kinematic viscosity and other thermal properties of air and water. All these properties are curve fitted and can be found in the appendix of this report.

- Fixed properties

Fixed properties are properties that do not change with differing weather conditions. These properties can be distinguished into three types; material bound properties dimensioning properties and selectable properties. Table 4 gives an oversight of all these properties, where they originate from and how they are related to a material.

Table 4 Parameters used in the simulation model

Parameter/property	Value	Unit	Comment/reference
Material bound properties	-	-	-
Conduction insulation	0.033	W/(m*K)	Conduction of polystyrene foam
Thermal emissivity glass	0.88	-	Emissivity of smooth uncoated glass
Glass transmittance	0.92	-	Transmittance of smooth uncoated glass
Plate emissivity	0.8	-	Value given is for c-Si PV. Emissivity for different PV types is estimated by Santbergen et al (Santbergen, Rindt, Zondag, & van Zolingen, 2010)
Conduction PV laminate	84	W/(m*K)	(de Vries, 1998)
PV reference efficiency	0.1358	-	Value given is for c-Si PV (Santbergen, Rindt, Zondag, & van Zolingen, 2010)
PV temperature coefficient	0.0045	K^{-1}	Value given is for c-Si PV (Santbergen, Rindt, Zondag, & van Zolingen, 2010)
PV effective transmittance-absorption product	0.835	-	Value given is for c-Si PV. Value is measured for different types of PV by Santbergen et al (Santbergen, Rindt, Zondag, & van Zolingen, 2010)
Heat transfer coefficient between cell and absorber	45	$W/(m^2*K)$	Determined experimentally (de Vries, 1998)
Dimensioning properties	-	-	-
Length	1.00	m	Standard PV panel length
Width	1.60	m	Standard PV panel width
Tube diameter	0.01	m	This size is often used in literature. Total system will be optimized for this parameter
Collector tilt	0	°	Assumed that PV lies on a flat surface
Thickness insulation	0.07	m	This size is used in the developed prototype
Plate-cover distance	0.028	m	This size is often used in literature. Total system will be optimized for this parameter
PV laminate thickness	4	mm	Thickness of c-Si PV laminate
Bond thickness	1	mm	This size is often used in literature. Total system will be optimized for this parameter
Selectable properties	-	-	-
Flow rate	0.02	$kg/(s*m^2)$	This size is often used in literature due to a combination of good thermal performance and low pump power consumption. Total system will be optimized for this parameter
Water inlet temperature	283.15	K	This is the average tap water temperature in the Netherlands. It is assumed that the temperature is not linked to weather conditions.

Aside from these inputs the performance of the system is highly dependent on weather conditions. The steady state simulation model needs high-resolution

weather data to properly forecast the different outputs of the PVT system. In literature hourly data is often used and many studies conclude that this resolution is high enough to accurately simulate a flat plate solar collector (Nafey, 2005). Nonetheless in this report data with a timestamp of 10 minutes is used as this was available from the KNMI database and it improves the accuracy of the outputs since more weather fluctuations are included in the simulation model (KNMI, 2014). The data is obtained for one year (2013) from the KNMI weather station in Deelen and the following weather inputs are considered:

- Average wind speed in timestamp on 10 meter altitude measured in m/s
- Average solar radiation in timestamp on a flat plane measured in W/m^2
- Average ambient temperature in timestamp measured in K

The simulation model uses these input data to solve all adjusted Hottel and Whillier equations and since some properties are dependent on the output (such as water and air properties), the model has to solve these equations iteratively. After calculating each timestamp different outputs can be extracted to analyze the performance of the system:

- The useful thermal energy, Q_u
- The produced electrical energy, Q_e
- The thermal and electrical efficiency of the system, η_{ther}, η_e
- The temperature of the different components, $T_{g-m}, T_{p-m}, T_{air-m}, T_{i-m}, T_{i-o}$

After assigning the materials, dimensions and selectable properties, the total simulated system can be presented by a block diagram as displayed in Figure 10. This simulation model is used to calculate efficiency curves, as explained in the theory, for different designs, PV types and collector materials.

Figure 10 Total PVT simulation block diagram

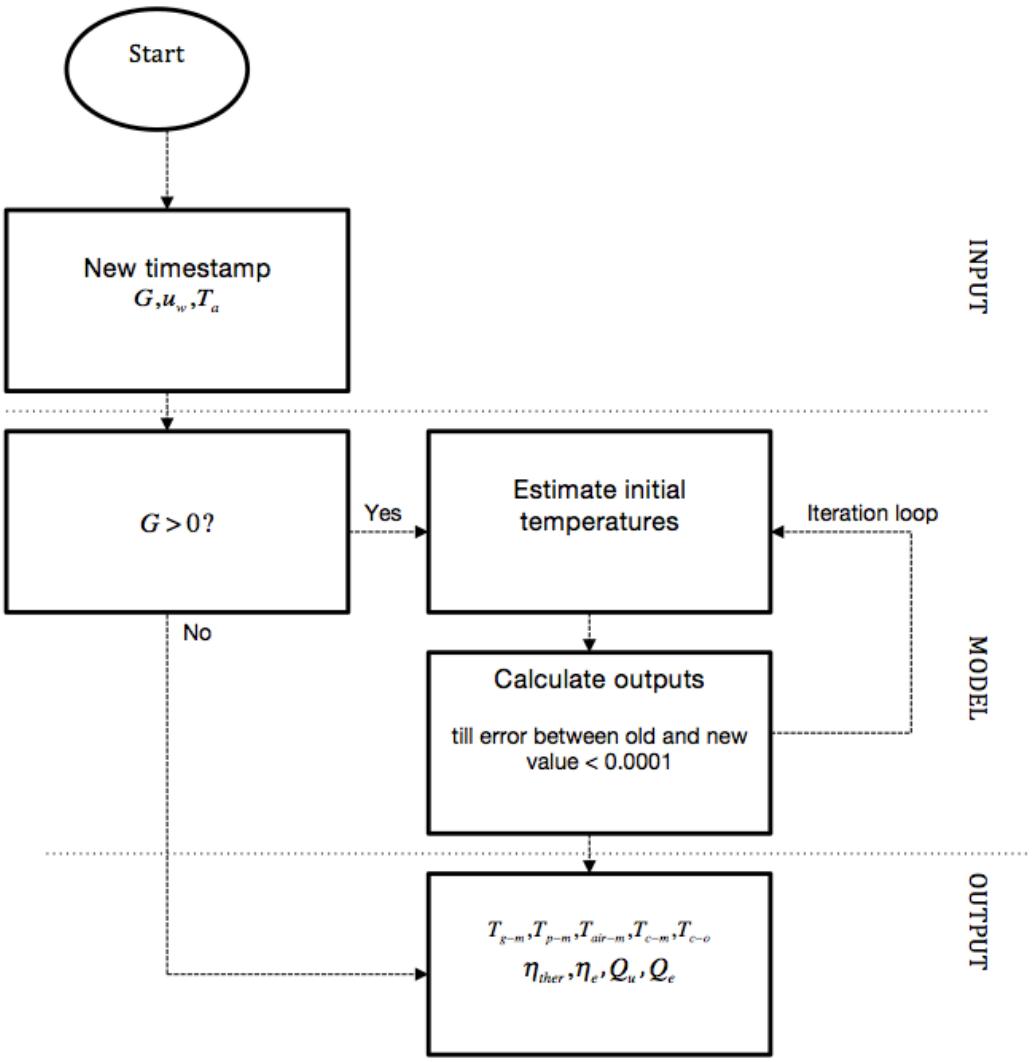

3.3.2 Storage tank

A storage tank, like the PVT system, needs to be simulated rather precisely since a too simple approach (such as assuming a fully mixed tank) can easily result in huge errors concerning the total performance of the PVT system with heat application. This is mainly because stratification plays a large role in storage tanks for solar collectors since this influences the temperature of the tapped water, the inlet temperature of the PVT collector and thus also the circulation pump operation scheme. Generally a higher stratification will result in lower temperatures in the bottom of the tank and this will increase the performance of a thermal collector. To simulate stratification the textbook of Duffie & Beckman is used for scientific background (Duffie & Beckman, 1991). The degree of stratification is dependent on multiple design choices such as size, location of inlets and outlets, flow rate from collector and flow rate from load.

A multi-nodal one-dimensional model is used that neglects horizontal temperature distributions. This model splits the tank in a certain amount of nodes that can exchange energy. It is shown that 10 nodes are sufficient for accurately simulating the stratification in a storage tank with low inlet and outlet flow rates (Cristofari, 2003). Additionally is it assumed that the inlets and outlets are fixed and the storage tank can be scaled up or down without affecting the stratification level. To use this model, some assumptions have to be made (Cruickshank, 2009):

1. The water flow in the tank is one-dimensional
2. The density and temperature is uniform and constant in each node over the time step
3. Water flows from each node are considered fully mixed before they enter neighboring node
4. The heat loss to the environment of the tank and conduction in the walls of the tank are low enough that 2D or 3D temperature gradients can be neglected
5. The flow rates are low enough that they do not promote extensive mixing within the storage tank

The energy balance equation on every node (i) is presented by the following equation:

$$m_i \frac{dT_{s,i}}{dt} = \left(\frac{UA}{C_p}\right)_i (T_{\backslash a} - T_{s,i}) + F_i^c \dot{m}_c (T_{c,o} - T_{s,i}) + F_i^L \dot{m}_L (T_{L,r} - T_{s,i}) + \begin{pmatrix} \dot{m}_{m,i}(T_{s,i-1} - T_{s,i}) & if - \dot{m}_{m,i} > 0 \\ \dot{m}_{m,i+1}(T_{s,i} - T_{s,i+1}) & if - \dot{m}_{m,i+1} < 0 \end{pmatrix} \quad (22)$$

$\dot{m}_i$ = mass of the water in node i
$T_{s,i}$ = temperature of the water in node i
t = time
UA = loss coefficient-area product of the storage tank
$\dot{m}_c$ = collector flow rate
$T_{c,o}$ = water temperature of the PVT outlet
$\dot{m}_L$ = load flow rate
$T_{L,r}$ = water temperature of the replenished or returned load

Where the first part of equation 22 calculates the losses (or gains) to the environment (often indoor temperature is used since storage tanks usually are placed inside a dwelling). The second part calculates the energy gains from the collector and the third part the energy losses to the load. In these parts a control function is used to determine which node receives water from the collector and which node receives water from the replenished load. Since the inlets and outlets are fixed these are defined as follows:

$$F_i^c = \begin{pmatrix} 1 & if - i = 1 \\ 0 & otherwise \end{pmatrix}$$
$$F_i^L = \begin{pmatrix} 1 & if - i = N \\ 0 & otherwise \end{pmatrix} \quad (23)$$

In the last part of equation 22 the energy balance between the nodes is calculated. In this equation a mixed-flow rate that represents the net flow into node i from node i-1 is used and is defined as follows:

$$\dot{m}_{m,1} = 0$$
$$\dot{m}_{m,i} = \dot{m}_c \sum_{j=1}^{i-1} F_j^c - \dot{m}_L \sum_{j=1+1}^{N} F_j^L \quad (24)$$
$$\dot{m}_{m,N+1} = 0$$

Ideally, the differential equation 22 is solved analytically since this would eliminate any inaccuracies resulting from numerical methods. Unfortunately the computing time associated with simultaneously solving multiple non-homogeneous differential equations is unacceptable and thus numerical techniques have to be used. A number of integration methods have been proposed for solving these kind equations (Newton, 1995):

- DIFFEQ, used in TRNSYS
- Runge-Kutta
- Backward Euler solution
- Forward Euler solution
- Crank-Nicolson solution

In the same study a comparison of these integration methods showed that the DIFFEQ and Crank-Nicolson solution performed best over a wide range of time steps. Both methods will be compared and the one with the smallest error will be used. This error can be obtained by calculating the shortage or surplus of internal energy in the storage tank over a year (52560 time steps of 10 minutes):

$$Error = \frac{\sum_{t=0}^{52560} Q_{t,loss-to-environment} + \sum_{t=0}^{52560} Q_{t,gain-from-collector} + \sum_{t=0}^{52560} Q_{t,loss-to-load} + U_{t=0} - U_{t=52560}}{\sum_{t=0}^{52560} Q_{t,solar-radiation}} \quad (25)$$

Q_t = energy fow at a certain timestep

U_t = internal energy of the storage tank at a certain timestep

If equation 22 was solved analytically, the outcome of equation 25 should be zero since it must follow the law of conservation of energy.

3.3.3 Condensing boiler and heat pump

As clarified before, multiple applications (presented in Table 2) are modeled in a way that they can use the produced heat from the PVT and upgrade it by means of an auxiliary boiler (gas-fired condensing boiler) or heat pump to fulfill a certain heat demand (DHW or low temperature space heating). Also the reference cases, which will be further explained in section 3.5, are equipped with a gas-fired condensing boiler or a heat pump. In the reference cases they use tap water and ground water as water source and heat source respectively.

Both models are based on a simulation model used in EnergyPlus. EnergyPlus is an open-source energy analysis and thermal load simulation program developed by the Office of Energy Efficiency and Renewable Energy (EERE) that is able to accurately simulate all kind of heating, ventilation and air conditioning systems (EERE, 2013).

Condensing boiler

The simulation model for the condensing boiler for DHW is based on a curve fit model that fits a normalized condensing boiler efficiency equation dependent on inlet temperature and part load ratio (PLR) with experimental data. This data is originating from two gas-fired condensing boilers produced by the company Viessman. The normalized efficiency curve is best fitted using a biquadratic function as shown below (EnergyPlus, 2013):

$$\eta_{norm} = A_0 + A_1 * PLR + A_2 * PLR^2 + A_3 * T_{w,in} + A_4 * T_{w,in}^2 + A_5 * PLR * T_{w,in} \quad (26)$$

PLR = fraction of the maximum heat producing capacity of condensing boiler
$T_{w,in}$ = temperature of the water leaving the condensing boiler

In this equation the PLR is defined as the fraction of the maximum heat producing capacity of the condensing boiler that is deployed in a certain time step. The set of different coefficients (A_0-A_5) are determined by the generalized least square method to fit the experimental data. To calculate the gas consumption (in Joule) the normalized efficiency has to be multiplied by nominal thermal efficiency (as calculated by EnergyPlus, value is 0.89), which is defined by the efficiency relative to the higher heating value (HHV) of fuel at a PLR of one. This is shown by the equation below:

$$Fuel = \frac{Capacity / \eta_{nom}}{\eta_{norm}} \quad (27)$$

The capacity of the condensing boiler is determined by the timestamp with the highest heat demand in the load profile (which will be explained later in this chapter). Since the efficiency is not known beforehand, a first guess is needed to estimate the gas consumption. After this step the precise capacity can be calculated iteratively.

Heat pump

To simulate the performance and outputs of a heat pump, a simulation model developed by the Oklahoma State University is used (Tang, 2003). This model is comparable but slightly more complex than that of the condensing boiler. Variables (that can vary every time step) influencing the performance of the heat pump are:

- Load side inlet water temperature, $T_{L,in}$
- Source side inlet temperature, $T_{S,in}$
- Load side water flow rate, V_L
- Source side water flow rate, V_S

The performance of a heat pump is split into an equation for the heat production and power consumption respectively:

$$\frac{Q_h}{Q_{h,ref}} = B_0 + B_1\left[\frac{T_{L,in}}{T_{ref}}\right] + B_2\left[\frac{T_{S,in}}{T_{ref}}\right] + B_3\left[\frac{V_L}{V_{ref}}\right] + B_4\left[\frac{V_S}{V_{ref}}\right] \quad (28)$$

$$\frac{Power_h}{Power_{h,ref}} = C_0 + C_1\left[\frac{T_{L,in}}{T_{ref}}\right] + C_2\left[\frac{T_{S,in}}{T_{ref}}\right] + C_3\left[\frac{V_L}{V_{ref}}\right] + C_4\left[\frac{V_S}{V_{ref}}\right] \quad (29)$$

In the equations the heat pump input variables are divided by reference values. For the reference temperature a value of 283 K is used. For the flow rates the maximum source and load flow rates of the evaluated heat pump are used. The heat production reference is the maximum heat production of the heat pump and the power consumption reference the maximum power capacity. Again these equations are used to compute the performance coefficients (B_0-B_4 and C_0-C_4) using the generalized least square method to fit experimental data. In this case manufacturers data is used from different heat pumps produced by the company Carriers. In this thesis an additional optimization step is performed in the case a heat pump has multiple flow rate modes, it choses the flow rate with the highest COP. Also an iteration step is needed to determine the correct water properties. This is needed since the output of the heat pump model functions as an input for the storage tank model as this system is closed (which is not the case with the condensing boiler for DHW as this system is open). Just as with the condensing boiler, the capacity of the heat pump is determined by the time step with the highest heat demand in the load profile. After setting all reference values, the modeling procedure can be illustrated using a block diagram (Figure 11). Note that the temperature of the source is determined by the PVT collector.

Figure 11 Total heat pump simulation block diagram

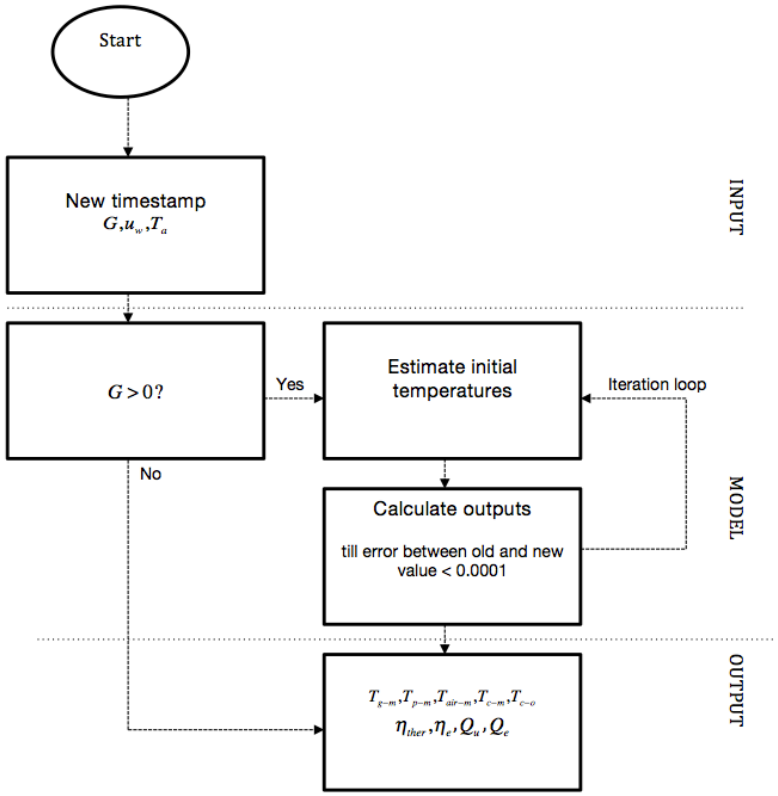

3.3.4 Additional equipment

In the total system additional equipment is necessary to couple the different components. As explained before, the fluid circulating in the PVT collector has to be antifreeze and therefore a heat exchanger is needed in order to transfer the heat to usable tap water. Aside from heat exchangers also circulating pumps are required to circulate the fluids and a control scheme has to be in place that turns the pump on or off. Heat losses in pipes and ducts are neglected in this report.

Heat exchanger

Duffie and Beckman have presented a way to combine the heat exchanger equations with the Hottel and Willier equations into a single equation that has the same form as collector equation 19 (Duffie & Beckman, 1991). This equation has an adjusted and somewhat lower heat removal factor since the heat exchangers does not transfer all heat from the PVT collector. To combine the equations, first the useful energy gain must be expressed in a different way:

$$Q_u = \dot{m} C_p (T_o - T_i) \tag{30}$$

Now the heat exchanger performance can be expressed in terms of its effectiveness:

$$Q_{HX} = \varepsilon (\dot{m} C_p)_{\min} (T_{PVT,o} - T_i) \tag{31}$$

Where ε represents the effectiveness of the heat exchanger and the min indicates the smaller of the fluid capacitance rates (collector side or tank side). By combining these equations it is possible to define equation 19 with an adjusted heat removal factor $F_R^{'}$ and both equations are shown below:

$$F_R^{'} = F_R\left[1+\left(\frac{A_c F_R U_L}{\left(\dot{m}C_p\right)_c}\right)\left(\frac{\left(\dot{m}C_p\right)_c}{\varepsilon\left(\dot{m}C_p\right)_{\min}}-1\right)\right]^{-1} \tag{32}$$

Here the min term stands minimum and this equation choses the fluid that has the smallest heat capacity.

$$Q_u = A_c F_R^{'}\left[S - U_L(T_i - T_a)\right] \tag{33}$$

These equations are integrated into the PVT simulation model.

Circulation pump & control scheme

The power consumption of circulation pumps (collector side and tank side) have been calculated by determining the frictional pressure of the system (Garg & Agarwal, 1994):

$$Power = \frac{\dot{m}\Delta P}{\rho} \tag{34}$$

= pressure difference
= water density

$$\Delta P = \rho g(\delta h + \delta h_f + \delta h_{buoy}) \tag{35}$$

In equation 35 δh is the head loss due to frictional resistance δh_f is the head loss due to fittings and bends and δh_{buoy} is the head loss due to buoyancy effects of the hot water and height different between storage tank and collector. This last term is neglected since it contributed only marginally to the total pressure loss. The other equations can be defined as follows:

$$\delta h = \frac{512}{D * g * \mathrm{Re}}\left(\frac{\dot{m}}{\rho * \pi^2 * D^2}\right)^2 \tag{36}$$

$$\delta h_f = K_f \frac{\left(\frac{\dot{m}}{\rho * \pi^2 * D^2}\right)^2}{32g} \tag{37}$$

In equation 37 K_f is a constant, which differs for different kind of fittings such as elbows, globe valves, gate valves and other fittings.

For the control scheme a realistic scenario is chosen: a control scheme based on the temperature difference of the outlet temperature of the PVT collector and the water temperature in the bottom of the storage tank. For flat plate solar collectors a standard temperature difference of 8 K activates the circulation pump and when this difference is below 4 K the pump is turned off. Since the PVT collector does not achieve such high temperatures as flat plate collectors, these boundaries have been investigated and optimised.

3.4 Load modelling

Goal of this research is to model the annual yield of PVT collectors with three different applications: preheating DHW, preheating low temperature central heating and a combination of both. The model is structured in a way that all simulated components need a certain input and give a certain output. As explained in the previous section, heat pumps and condensing boilers need two types of input in every timestamp; the state of the water present in the storage tank that they use as input; and the heat demand in that timestamp. This section explains how this heat demand is determined. For both DHW and low temperature central heating, demand patterns are based on three different households; a large energy consumer; a medium energy consumer and a small energy consumer. Information concerning these households is further specified in Table 5 and is based on a anonymous database, provided by Alliander, including building information, hourly gas and electricity consumption patterns and household information. Additionally information from VROM is used for determining which fraction of gas consumption goes to different applications (heating, DHW and cooking) (PRC Bouwcentrum BV, 2004).

Table 5 Specifications concerning heat patterns of three different households

Consumer type	**Large consumer**	**Medium consumer**	**Small consumer**
Dwelling type	Detached	Semidetached	Terraced
Family type	Pair with children	Pair without children	Single
Year of construction	<1940	1980-1990	1980-1990
Energy label	G	A	A
Total gas consumption (m^3/year)	4056	2288	1351
Average gas consumption part for DHW (m^3/year)	443	340	235

3.4.1 DHW load

The DHW load is modelled with a special program that is developed by the University of Kassel especially for solar thermal simulation models to replace the relatively simple and standardized draw-off patterns (Jordan & Vajen , 2005). This program ‘DHWcalc’ has multiple advantages with respect to standardized draw-off patterns and these are summarized below:

- It can produce datasets based on household data (amount of people, amount of kids, presence of a bath or shower)
- It is possible to adjust the time step duration while generating DHW load profiles (daily, hourly, sub hourly, 10 minutes, etc.)
- Load profiles can be normalized with yearly heat consumption data
- Uses realistic probability distribution loads and flow rate distributions (see Figure 12) enabling it to more accurately investigate yearly yields of solar systems that preheat DHW instead of one standardized pattern
- Possible to simulate extreme events (long holidays, very high draw-off patterns and extremely large daily variations in draw-off patterns)

Figure 12 Realistic probability distribution loads and flow rate distributions used in DHWcalc (Jordan & Vajen , 2005)

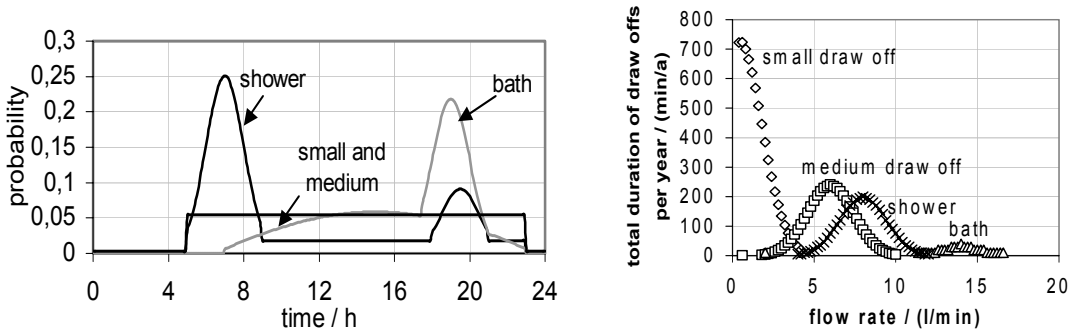

The program is used, based on data provided in Table 5, to calculate draw-off patterns for three different households and these patterns are used as load profiles in the PVT and heat application model. The hot tap water temperature is fixed at 60 ° C since this is necessary to comply with legislation due to protection against legionella. DHW flow patterns of the three households are shown in

Figure 13 as an example.

Figure 13 The DHW load profile of three different households in a week in January

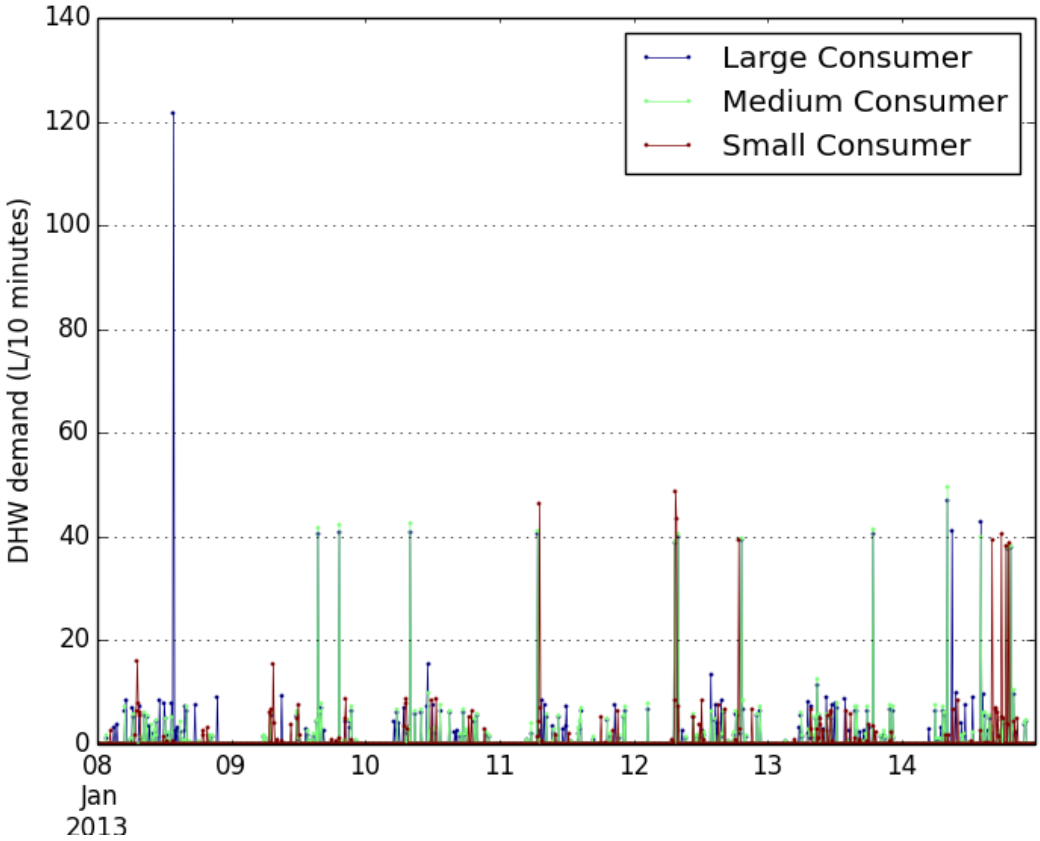

3.4.2 Low temperature heating load

The low temperature heating load profiles used in this report originate from hourly gas profiles provided by Alliander. It is assumed that the daily patterns of gas and heat consumption are equal and research has pointed out that this is a valid assumption for Dutch households (Houwing, Negenborn, & de Schutter, 2011). Still this assumption leads to some noise in the dataset, especially caused by peaks as a result from large DHW draw-offs.

Three datasets have been chosen that matches the three different consumer types as described in Table 5. It is assumed that the heat generation system (condensing boiler, heat pump, district heating) has no significant influence on the hourly heating profile since heat demand is mainly driven by the thermostat control system. Still to obtain the heat demand, the hourly gas consumption profile is translated to a heat demand using the condensing boiler model described in the previous section. This translation resulted in an additional assumption, namely that all three households generated heat with a condensing boiler. This seems like a valid assumption since around 80 % of all Dutch households use condensing boilers and the gas profile of the households supported this assumption (VFK, 2012). In Figure 14 the normalized (fraction that is consumed for heating) heat demand profile is presented and this profile is interpolated to timestamps of 10 minutes.

Figure 14 The heat demand profile of three different households in a week in January

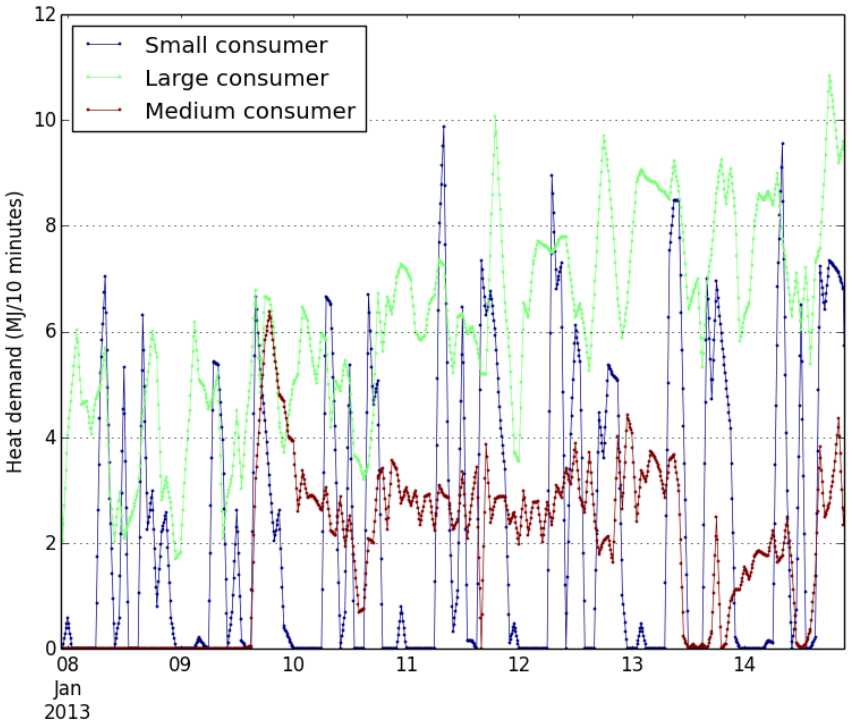

3.5 Validation and optimization

In this section the validation and optimisation methods are described. The starting point of this section is to obtain a set of fixed properties for three PVT collectors:

1. The prototype PVT collector that is developed within the Nanosol project
2. An economically optimised glazed PVT collector
3. An economically optimised unglazed PVT collector

With these three PVT collectors all different system configurations are optimised. Also a method is presented for the validation of the steady state model by using experimental data that is obtained by DNV GL.

3.5.1 Validation of the simulation model

The simulation model is validated using experimental data for one day with a minute interval time series. For this experiment, an unglazed PVT collector is constructed by attaching a 0.34 m^2 solar panel developed by Hyet Solar to a polypropylene (PP) channel system due to strong double-sided tape. This system is attached to a PP header and tubing system and is powered by a water pump. A small and compact weather station is attached on the frame together with different measuring devices. The total experimental setup can be seen in Figure 15. The following parameters have been measured every minute:

- Inlet temperature (K)
- Outlet temperature (K)
- Ambient temperature (K)
- Incoming solar radiation (J/m^2)
- Wind speed (m/s)
- Load current (A)
- Load voltage (V)
- Resistance (mΩ)

Figure 15 Experimental setup measuring the PVT collector prototype

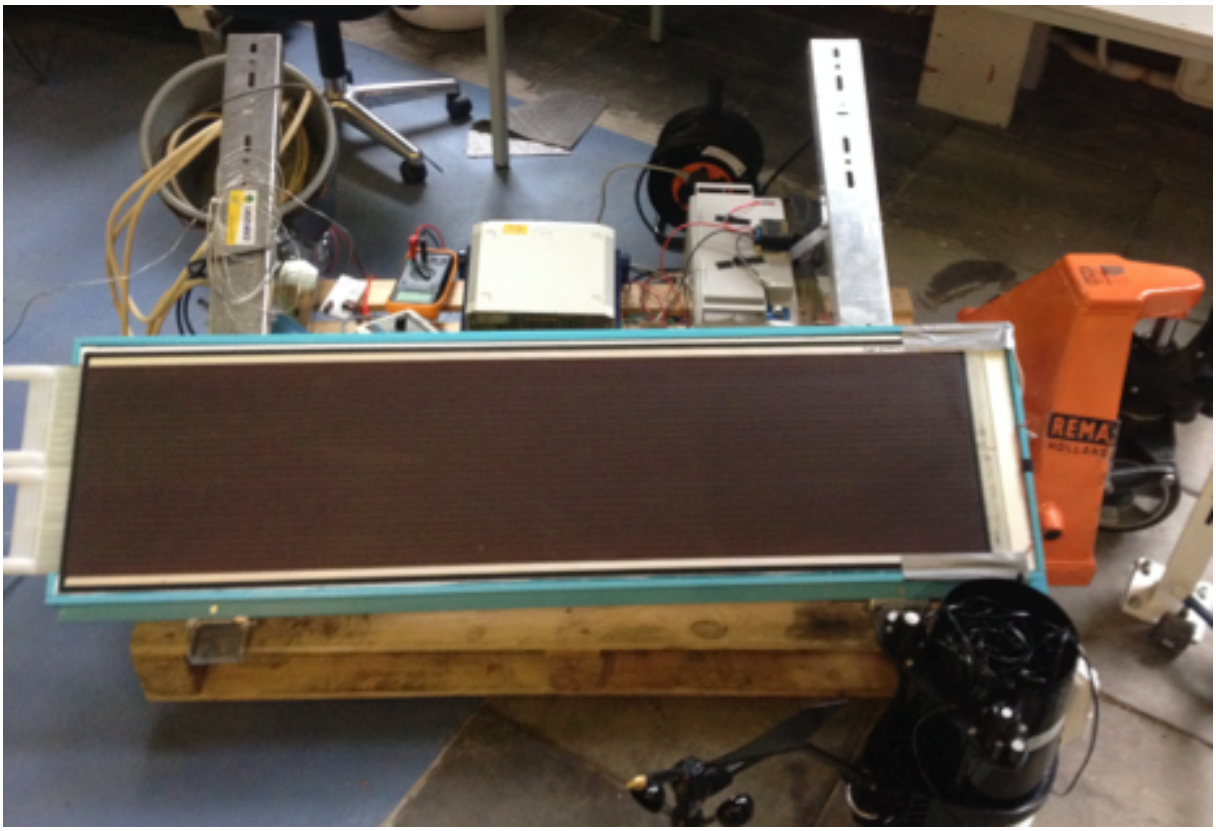

In the simulation model all fixed parameters, such as dimensioning parameters and flow rate, are assigned to the PVT collector and unknown parameters are estimated. These unknown parameters included:

- Plate emissivity
- Effective transmittance-absorption product
- Bond conduction
- PV temperature coefficient
- PV reference efficiency
- Conduction insulation

The experiment is carrier out on the 19th of May, on a day with very high fluctuating solar radiation. The circulation pump is controlled to pump water with a flow rate of 0.01 kg/s through the PVT collector.

In the next step, the collected weather data from the experiment is used as input in the PVT simulation model. These results are compared with the experimental results to obtain the deviations between model and experiment. Two methods have been used for comparing both results: the correlation coefficient (r) and the root mean square percent deviation (e). These equations are evaluated for both electricity production and heat production and are shown below:

$$r = \frac{N\sum X_i Y_i - \left(\sum X_i\right)\left(\sum Y_i\right)}{\sqrt{N\sum X_i^2 - \left(\sum X_i\right)^2}\sqrt{N\sum Y_i^2 - \left(\sum Y_i\right)^2}} \quad (37)$$

X_i = experimental result at timestep i

Y_i = simulated result at timestep i

$$e = \sqrt{\frac{\sum (e_i)^2}{N}} \quad (38)$$

e_i is defined as:

$$e_i = \left[\frac{X_i - Y_i}{X_i}\right] * 100 \quad (39)$$

Since many parameters could not be determined before the experiment, a script is written that performs an optimisation. In the first guess and range of the fixed parameters are presented that could not be determined beforehand (Table 6). These parameters are fitted with the script using the minimum of the product of equation 37 and 38 for electricity production and heat production combined as best fit.

Table 6 Fixed parameters fitted with experimental data

Parameter/property	First guess	Unit	Range
PV reference efficiency	0.062	-	0.4-0.9
PV temperature coefficient	0.002	K^{-1}	0.001-0.0045
Heat transfer coefficient between cell and absorber	20	$W/(m^{2*}K)$	5-80
Plate emissivity	0.8	-	0.7-0.9
PV effective transmittance-absorption product	0.835	-	0.7-0.9
Conduction insulation	0.033	W/(m*K)	0.01-0.05
Bond thermal conduction	0.2	W/(m*K)	0.005-0.05

3.5.2 Optimization of PVT collector and sensitivity analysis

Since many properties and parameters are design choices an optimization step is required to find the most optimal materials, dimensions and selectable properties. The optimisation step of this multi-output system is based on two different goals and takes into account the allocation of the two different products; heat and electricity.

The two different goals are:

1. Cost-benefit analysis. The quantity where the optimisation is based on is the simple payback period (PBP) that includes the initial investment (I), the annual benefits (B) and costs (C) and is calculated using equation 40 (Blok, 2007).

$$PBP = \frac{I}{B - C} \tag{40}$$

I = initial investment
B = yearly benefits
C = yearly costs

2. Exergy analysis. This is a better allocation method than considering only energy since the value of electricity is much higher than heat (equation 41).

$$B = \left[1 - \frac{T_a}{T_o - T_a} * \ln\left(\frac{T_o}{T_a}\right) \right] * Q_u + Q_e \tag{41}$$

The economic value of produced heat can only be valuated when the annual heat production of a PVT collector is utilized. For this optimisation the heat is used for preheating DHW and the benefits are expressed as yearly saved gas consumption. In this optimisation procedure one PVT collector is evaluated and the following parameters are fixed:

- The PVT collector has an area of 1.00 m x 1.60 m (1.60 m^2)
- A heat exchanger with an effectiveness of 0.9 is used
- The volume of the storage tank is 300 L
- A large consumer DHW load profile is used
- A condensing boiler of 59 kW is used as auxiliary heater

Firstly, an optimisation is made based on dimensioning properties such as tube diameter and plate-cover distance (for glazed PVT collector). Secondly, an optimisation step is performed based on different materials changing the material bound properties as shown in Table 4. Four different PV types (p-Si Pin Up Module (PUM), p-Si Emitter-Wrap-Through (EWT), a-Si and CIGS) and two different collector types (copper and high-density-polypropylene (HDPE)) are evaluated. In this last step also the pump control scheme and the flow rate are optimized. In the optimization procedure it is important that all parameters are optimized and since different combinations of parameters have a specific influence on the result, parameters could not be optimized in isolation. A script is written that is able to vary all parameters, producing all possible combinations, and determine all local and global minima (payback period) and maxima (exergy).

The investment and variable costs are presented in Table 7. Note that a lot of prices (installation, integration, storage tank, pump and control system costs) are rather high since only one PVT collector is installed. The economic influence of the amount

of collectors is investigated in the next section. Also note that some prices where not up-to-date or are presented in other currencies. In these cases it is assumed that the real price is remained constant and inflation and currency rates are used for correction.

Table 7 Cost and price overview

Cost component (1.6 m^2)	Amount	Source
p-Si PV – PUM ($\eta_{e,ref} = 0.141$)	€ 157.9	(IRENA, 2013) (PV Magazine, 2014) (Santbergen, Rindt, Zondag, & van Zolingen, 2010)
p-Si PV – EWT ($\eta_{e,ref} = 0.152$)	€ 170.2	(IRENA, 2013) (PV Magazine, 2014) (Santbergen, Rindt, Zondag, & van Zolingen, 2010)
a-Si PV ($\eta_{e,ref} = 0.078$)	€ 56.2	(IRENA, 2013) (Santbergen, Rindt, Zondag, & van Zolingen, 2010)
CIGS PV ($\eta_{e,ref} = 0.111$)	€ 94.2	(IRENA, 2013) (Santbergen, Rindt, Zondag, & van Zolingen, 2010)
Inverter ($\eta = 0.95$)	€ 0.5/W_p	Cost function based on data provided by: (SMZ, 2013)
Installation costs	See Appendix	(SMZ, 2013) and based on solar collector tenders
Glass cover	56.17 €/m^2	(Kumar & Tiwar, 2009)
EPS insulation	4.2 €/m^2	(Hout & bouwmaterialen, 2011; PV Magazine, 2014)
Copper framework with tubes	€ 11.8	(Kumar & Tiwar, 2009)
Copper headers	€ 6.0	(Kumar & Tiwar, 2009)
HDPE framework with tubes	€ 4.7	(Pachkawade, Nimkar, & Chavhan, 2013)
HDPE headers	€ 2.4	(Pachkawade, Nimkar, & Chavhan, 2013)
Piping system	See Appendix	Based on solar collector tenders
Epoxy storage tank with heat exchanger coil	€ 488	Based on cost function (Rodríguez-Hidalgo, Rodríguez-Aumente , Lecuona, Legrand, & Ventas, 2012)
Two circulation pumps	€ 40.0	(Kumar & Tiwar, 2009)
Pump control scheme	€ 20.0	(Rodríguez-Hidalgo, Rodríguez-Aumente , Lecuona, Legrand, & Ventas, 2012)
Additional PVT integration costs unglazed	€ 24.5	(Bakker, Zondag, Elswijk, Strootman, & Jong, 2004)
Additional PVT integration costs glazed	€ 49.0	Assumption
Electricity price (including taxes)	€ 0.063/MJ	Based on different offers by energy suppliers
Electricity price (after netting boundary)	€ 0.013/MJ	Based on different offers by energy suppliers
Gas price (including taxes)	€ 0.017/MJ	Based on different offers by energy suppliers

After all optimisation steps, the optimum glazed and unglazed PVT collector are determined and several parameters are tested using a sensitivity analysis.

3.5.3 Optimization of total system

To answer the research question, all different system configurations as described in and Table 2 are evaluated. In contrast to the previous section, the dimensions of all components must be variable to determine the most optimal one. Three different PVT collectors are evaluated; the economic optimal unglazed PVT collector, the economic optimal glazed PVT collector and the prototype. Also three different households are examined as it is expected that the fluctuation and characteristics of load profiles for DHW and low temperature heating may have influence on the annual yield of the total system. For the optimisation of the systems different scripts are written and these are explained for all system configurations.

Preheating DHW

In this system several dimensioning and capacity parameters are evaluated and optimised based on a simple payback period (equation 40). The additional investment costs of the different components are modelled dynamically using costs functions (see Appendix). All other prices are presented in Table 7 and are linearly correlated with PVT collector area. It is assumed that every household already possesses a condensing boiler. Also the inside temperature must be since there is energy transfer between the storage tank and the ambient. This temperature is assumed to be 20 °C.

Figure 16 shows how the optimisation procedure works. The dimensioning and capacity parameters that are varied are:

- PVT collector area (range 1.6-32 m^2)
- Storage tank volume (range 100 L-1500L)
- Degree of stratification (range 4 nodes – 10 nodes)
- Flow rate (range 0.001-0.05 kg/(s*m^2))
- Pump control scheme (range $\Delta T_{on} = 4 - 8K$, $\Delta T_{off} = 1 - 3K$ and $(\Delta T_{off} + 2) < \Delta T_{on}$)

The modelling procedure is shown in Figure 16 and this procedure is repeated for 52560 time steps (one year). The varying parameters that are object for optimisation determine the investment costs and with this information a simple payback period can be calculated. The optimisation script varies all five parameters three times in the specified range (producing 5^3 = 125 results). The parameters associated with optimum result are than selected (with the lowest payback period) and the procedure is repeated with a smaller range around the selected parameters. Eventually the optimisation script converges to a minimum payback period. This is done for the three defined consumers and a sensitivity analysis is eventually performed where certain isolated parameters are varied.

Figure 16 Simulation block of the PVT system applied for preheating DHW

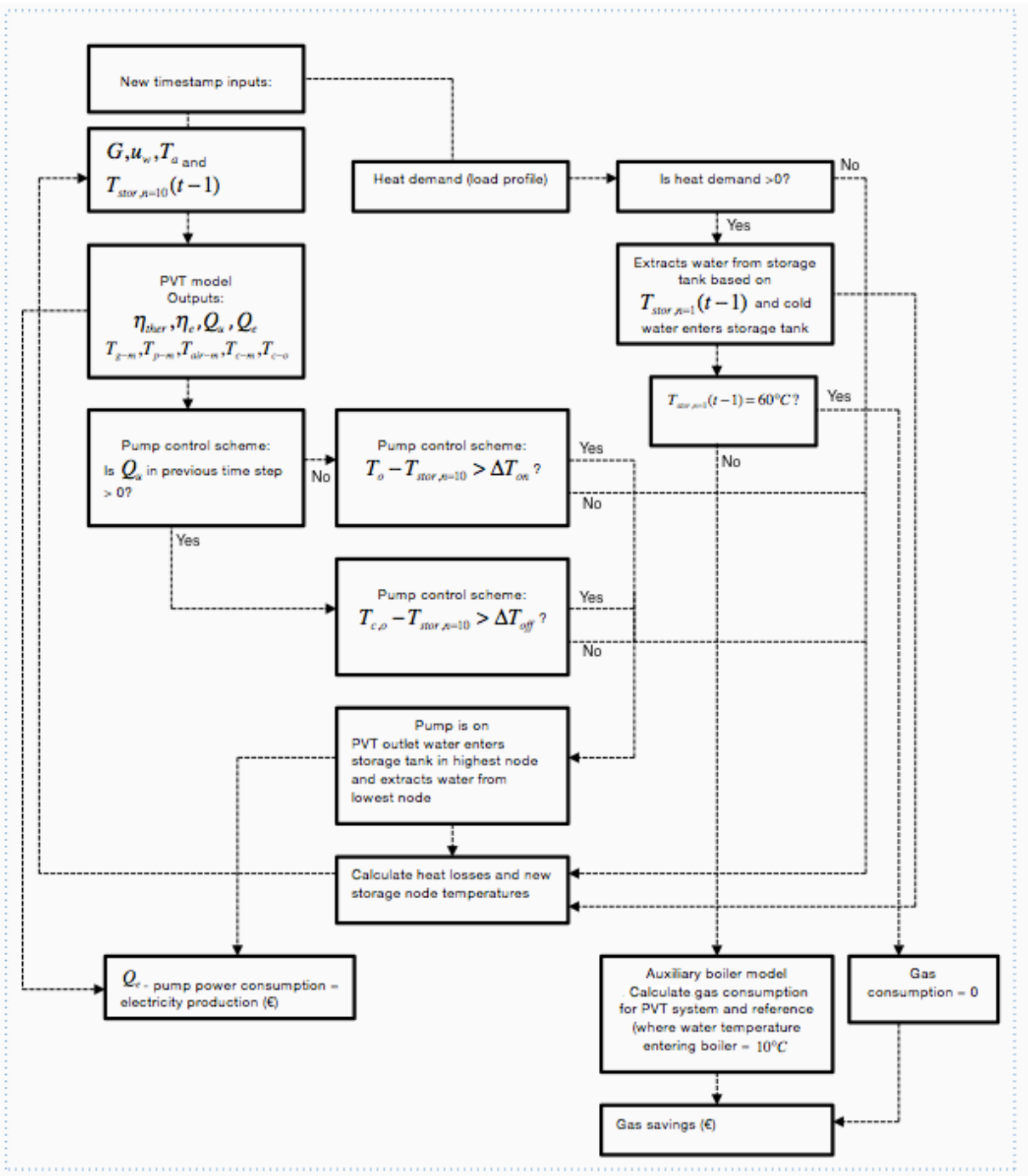

In the reference scenario all households are equipped with a condensing boiler that uses tap water of 10 °C as input.

Preheater heat pump for low temperature space heating

Again, the optimisation procedure is based on minimizing the simple payback period. The additional investment costs of the different components are modelled dynamically using costs functions (see Appendix). All other prices are presented in

Table 7 and are linearly correlated with PVT collector area. It is assumed that every household already possesses a condensing boiler that can be used for low temperature space heating when the heat pump cannot cover full demand. Since in this system configuration a PVT collector and storage system replace the ground water closed loop that is normally used as heat source for a water-to-water heat pump, a reference scenario is defined that equips an identical heat pump in combination with a ground water closed loop system. Another reference scenario is used where the three households only use a condensing boiler to fulfil their low temperature central heating demand. Since this system has a larger heat demand than the DHW system, this could potentially lead to more required PVT area, therefore a netting boundary is set on 5000 kWh. After this boundary, households receive 0.05 €/kWh for their produced electricity.

The optimisation procedure is presented in Figure 17 and the following dimensioning and capacity parameters are varied:

- PVT collector area (range 4.8-64 m^2)
- Underground storage tank volume (range 500 L-8000L)
- Degree of stratification (range 4 nodes – 10 nodes)
- Flow rate (range 0.005-0.2 kg/(s*m^2))
- Pump control scheme (range $\Delta T_{on} = 4 - 8K$, $\Delta T_{off} = 1 - 3K$ and $(\Delta T_{off} + 2) < \Delta T_{on}$)
- Heat pump capacity (20-100% central heating maximum demand coverage)
- The minimum acceptable storage tank temperature for operation heat pump (5-15 °C)

The inlet temperature of the heat pump is fixed on 30 °C since the application is for low temperature heating. Further, it is assumed in this model that the large underground storage tank can be modelled in the same way as in the previous model. The ambient temperature that must be estimated, since energy transfer occurs between the storage tank and the ambient, is set on 10 °C. The same modelling procedure, described in the previous section, is used to optimise all parameters. Also a sensitivity analysis is performed to investigate the influence of the different parameters in isolation.

Figure 17 Simulation block of the PVT system applied for preheating water for heat pump

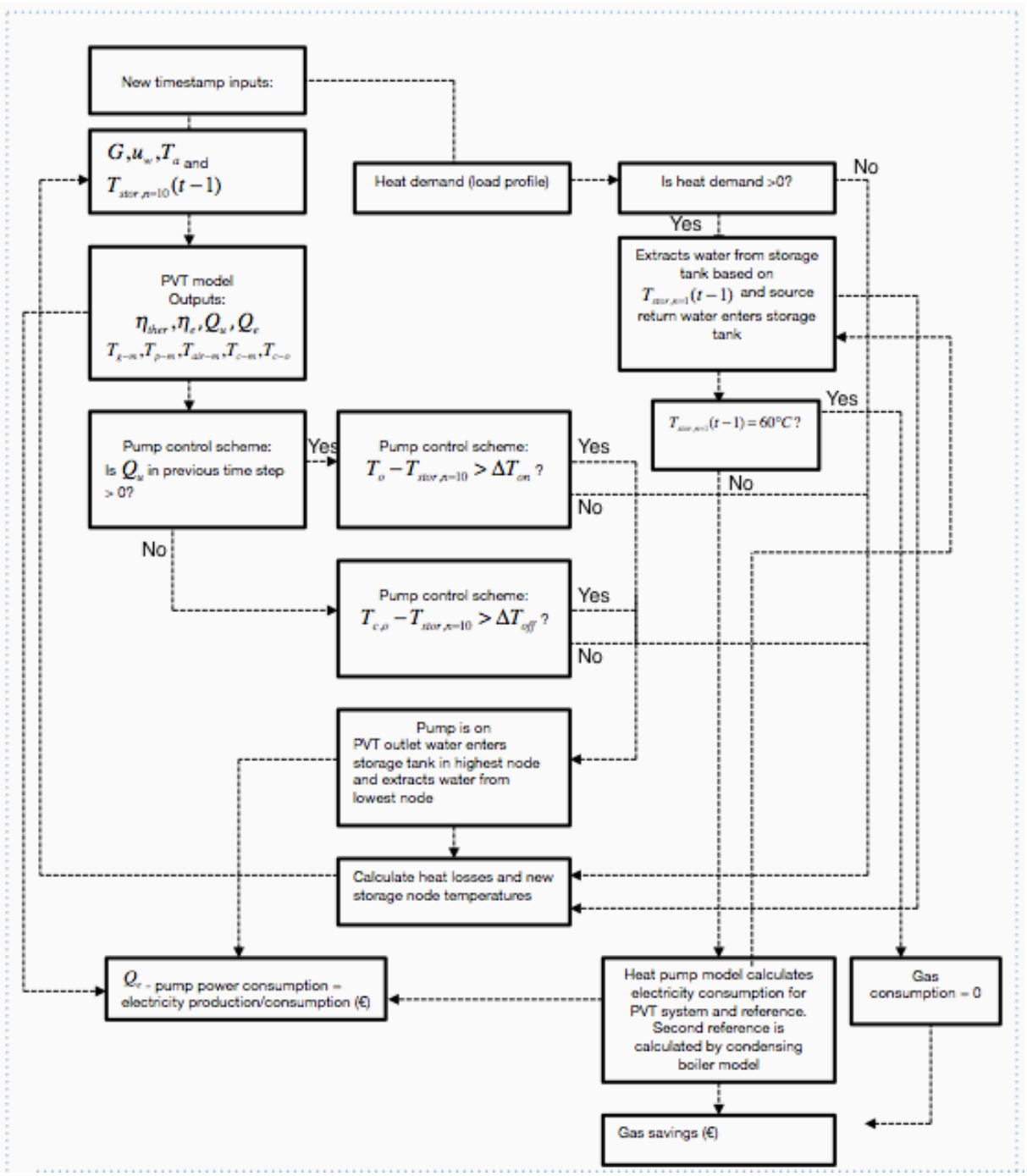

Preheater for DHW and heat pump for low temperature space heating

The last configuration consists of a combination of both applications. The rationale behind this configuration is that more heat can be utilized during different periods; utilization of heat for the heat pump in heating periods and utilization of heat for DHW in summer periods. This model integrates the previous described models into one and a certain control scheme determines when the collector flow will fuel the

storage tank used for preheating the heat pump and the storage tank used for preheating DHW. Since higher temperatures are obtained more frequently in summer periods when heat demand is low (and DHW demand is still high), a temperature boundary will function for switching the flow to fuel the heat pump storage tank or DHW storage tank. The control scheme switches to fuelling the DHW tank if the average heat pump storage tank reaches a certain temperature or if the outlet temperature of the water is higher than the outlet temperature of the heat pump.

4 Results

The results will be presented in the same order as in the methods section. Firstly, the PVT model will be evaluated using efficiency curves. Secondly, the storage tank model will be investigated. Thirdly the PVT model will be evaluated using experimental data. Fourthly, the PVT collector will be optimised based on annual yields and lastly, three different system configurations will be evaluated and optimised. It is important to note that when certain parameter or property values are not specified, the values presented in Table 4 are used.

4.1 PVT model

In this section, different PVT systems are analysed, compared with other references and the influence of different PVT components will be investigated. For flat plate thermal collectors and PVT collectors, the common way to compare different types is by using thermal efficiency curves. For a fair comparison, some conditions are fixed while generating the thermal efficiency curves. These conditions are identical to the reference scenario (Zondag H. , de Vries, van Helden, van Zolingen, & van Steenhoven, 2003):

- Flow rate (0.021 kg/(s*m^2))
- Solar radiation (800 W/m^2)
- T_a (20 °C)
- Wind speed (1 m/s)
- c-Si PV cells are used in the PVT collector ($\eta_{e,ref} = 0.097$, $\beta = 0.0045 K^{-1}$)

Figure 18 shows the thermal efficiency curves for different designs: channel, sheet-tube, glazed and unglazed. Also PVT collectors have been presented with a HDPE framework with tubes. As a reference also two copper sheet-tube (glazed and unglazed) have been presented scenario (Zondag H. , de Vries, van Helden, van Zolingen, & van Steenhoven, 2003).

Also electric efficiency curves are generated (without the reference) and are showed in the picture below (Figure 19).

Figure 18 Thermal efficiency curves: simulated compared with references

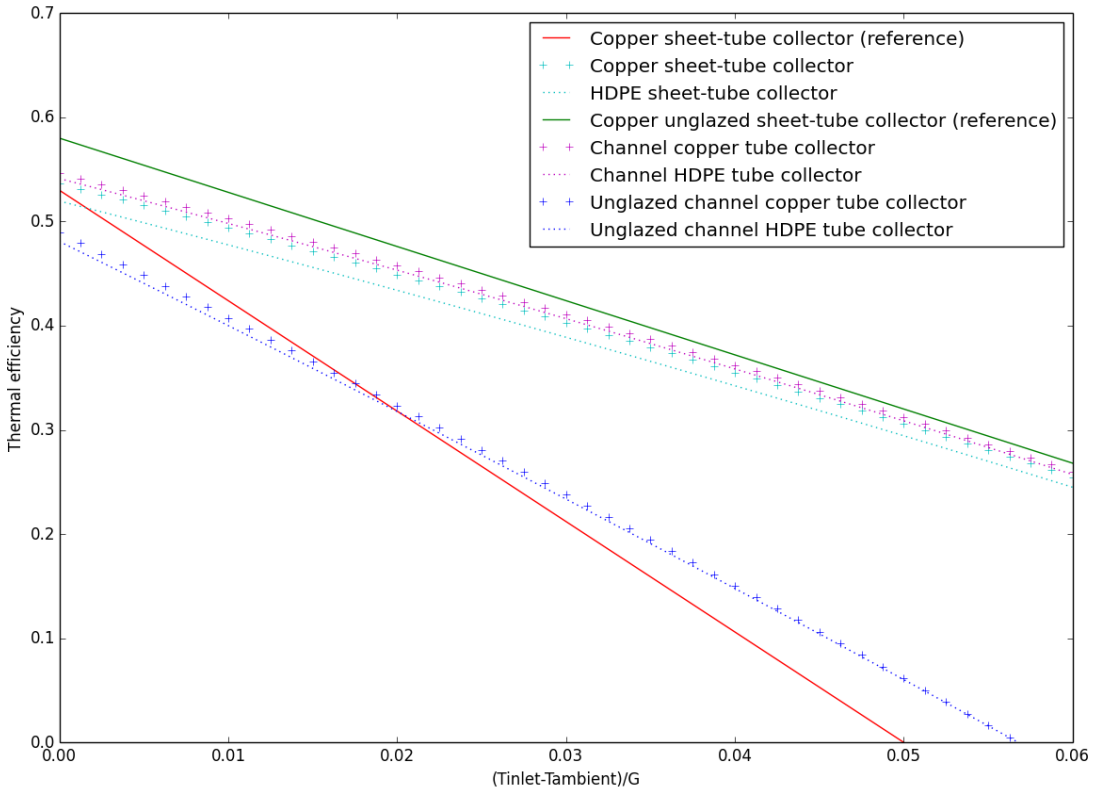

Figure 19 Electric efficiency curves

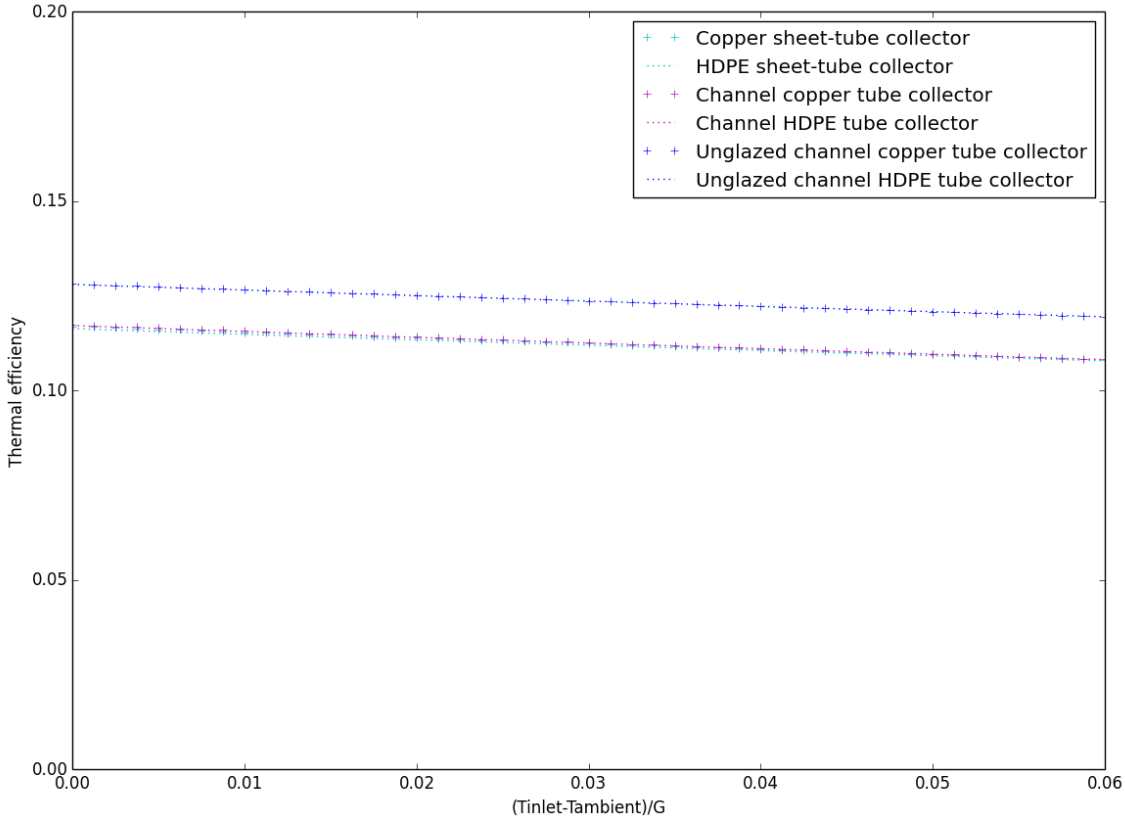

To see how the different PVT components influence the thermal efficiency, as explained in section 2.3.1, different efficiency curves have been plotted without certain PVT components. All PVT components will be replaced with components standardly used in flat plate solar thermal collectors. The following components will be replaced:

1. The PV is removed from the collector, which will result in higher thermal yields since there is no electricity production. Also the absorption factor of a PV-surface is lower and the surface is not spectrally selective.

2. The attachment between PV and collector is removed. The conduction of heat will be higher when this layer of glue and potential is removed.

The different effects are illustrated in Figure 20 for a copper glazed channel PVT collector. Note that the same conditions apply as in Figure 18.

Figure 20 Thermal efficiency curve of a PVT collector with and without PVT parts

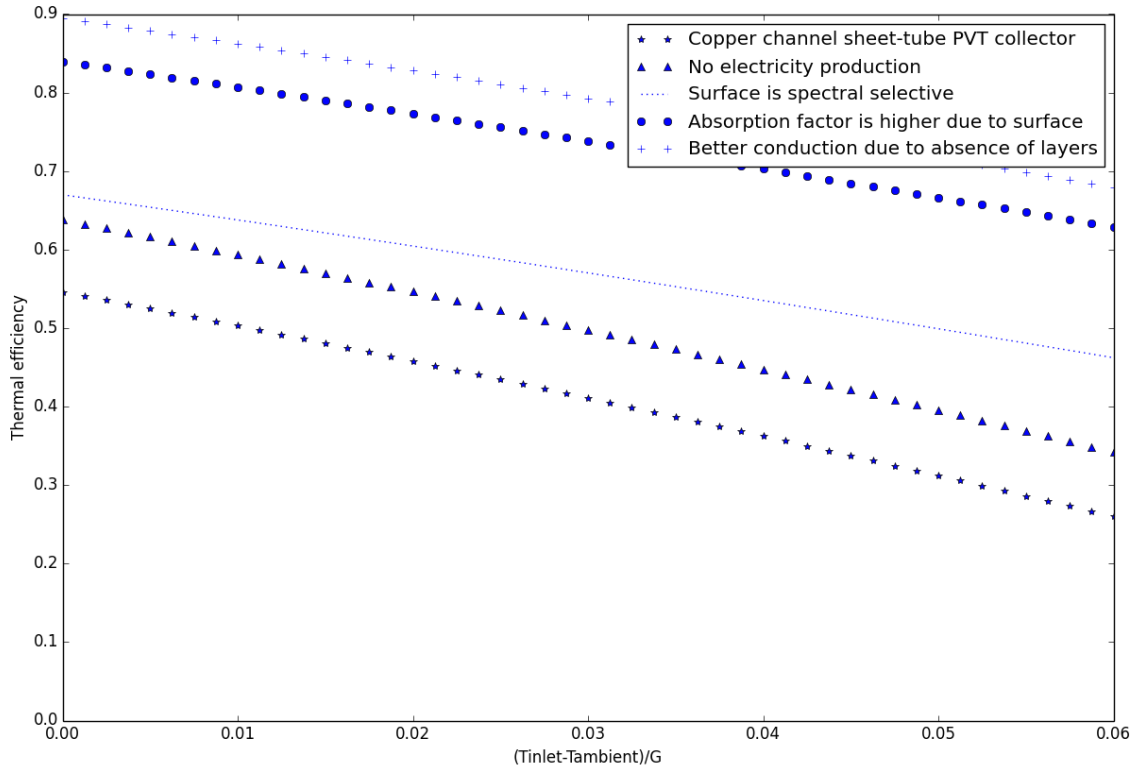

In the next step, a glazed channel PVT model is connected to a dataset with all relevant weather conditions in 10-minute timestamps. Figure 21 shows how the temperatures of the different components, ambient and fluid evolve over time using a flow rate of 2 kg/(s*m^2). Also the useful energy and the solar radiation are presented in this graph. No pump control scheme is used here and the PVT collector is not connected to a storage tank. The inlet temperature of the water is fixed at 10 °C and three days are evaluated (28, 29 and 30 May).

Figure 21 Evaluation of temperatures of different components, the useful thermal and solar energy

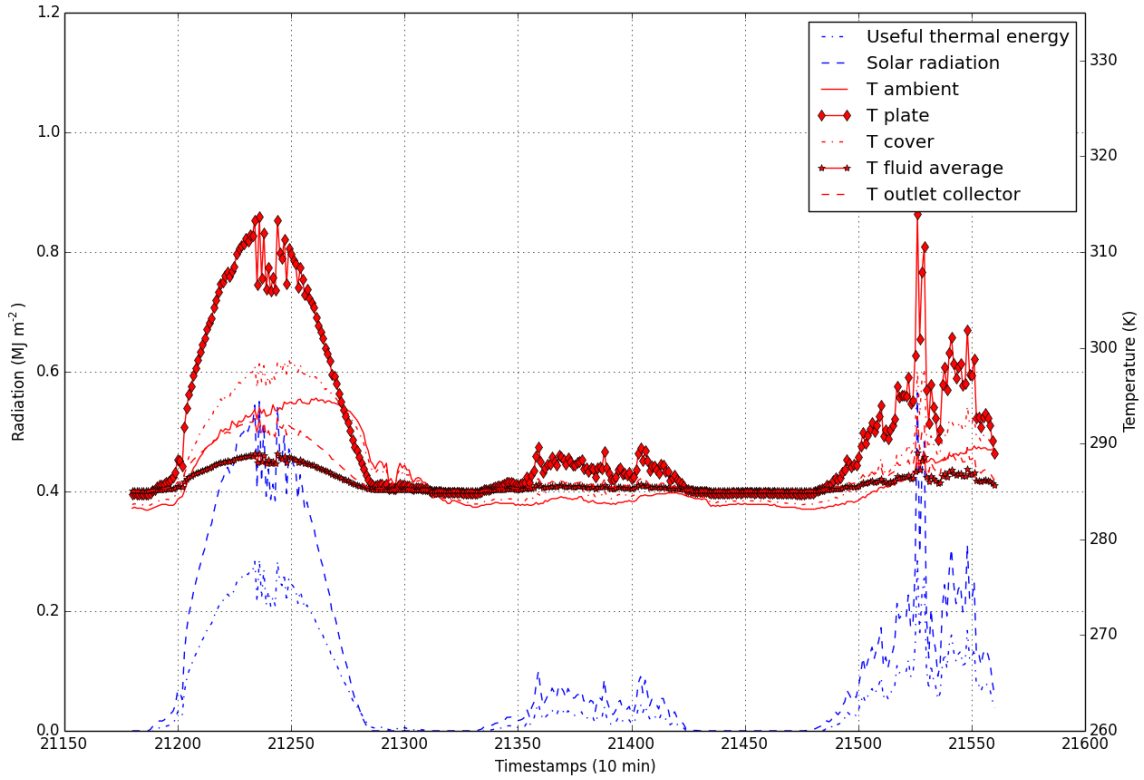

4.2 Storage tank model

The storage tank is modelled one-dimensionally and since an analytical solution is not possible, a numerical integration method must be used. Two numerical integration methods are identified as most suitable and these have been tested using equation 25. These methods have been tested for a total system with a load connected to it (for preheating DHW). The approximation of the integration method can become more uncertain when load flow rates, collector flow rates and storage tank size are not well dimensioned. The results are presented in Table 8, also the influence of the level of stratification on the error is displayed in this table.

Table 8 Errors for different system sizes as a result of the numerical integration methods

Integration method	**DIFFEQ**		**Crank-Nicolson**	
Level of stratification	4 nodes	10 nodes	4 nodes	10 nodes
Error (Volume = 300 L, Col. Area = 2 m^2)	-0.0056	-0.0085	0.0234	0.0428
Error (Volume = 300 L, Col. Area = 10 m^2)	0.0041	0.0067	0.0278	0.0513
Error (Volume = 600 L, Col. Area = 2 m^2)	-0.0297	-0.0100	-0.0305	-0.0103
Error (Volume = 600 L, Col. Area = 10 m^2)	0.0000	0.0005	-0.0002	-0.0013

The stratification is also analysed in detail. The assumption is that a more stratified storage tank will result in higher annual yields since the average fluid inlet temperature is lower resulting in higher thermal efficiencies. The analysis is performed using the DIFFEQ integration method, a storage tank with 300L volume and 2 m^2 of PVT collector area. The evaluated period is the same as Figure 21 and now the flow rates are presented on the left Y-axis (Figure 22 and Figure 23).

Figure 22 Temperature development through time for a 4-node storage tank

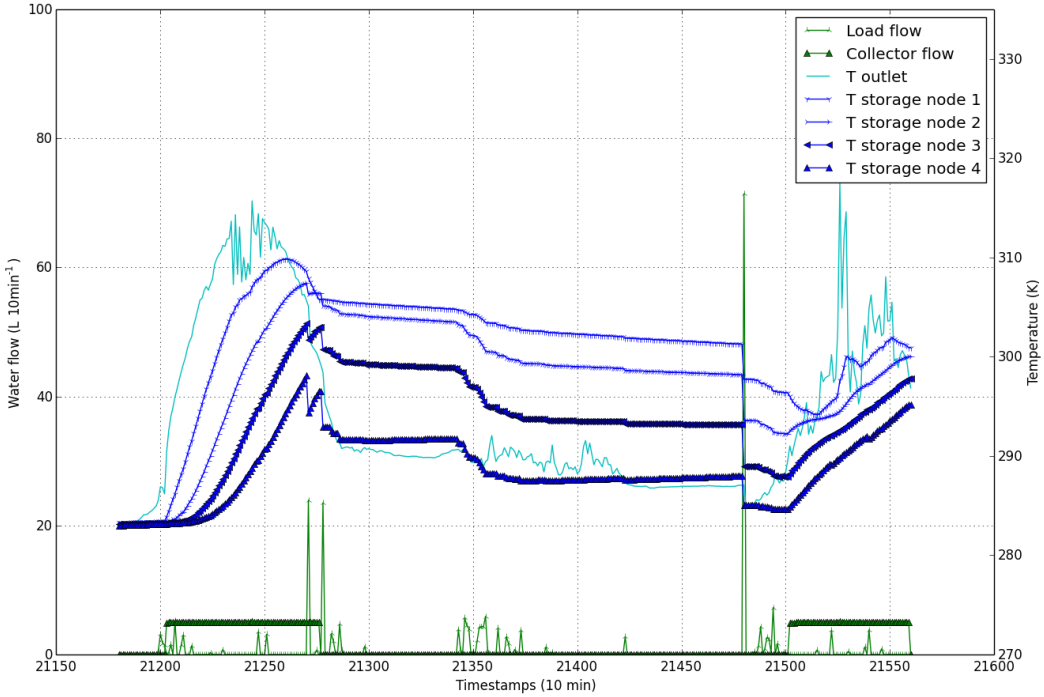

Figure 23 Temperature development through time for a 10-node storage tank

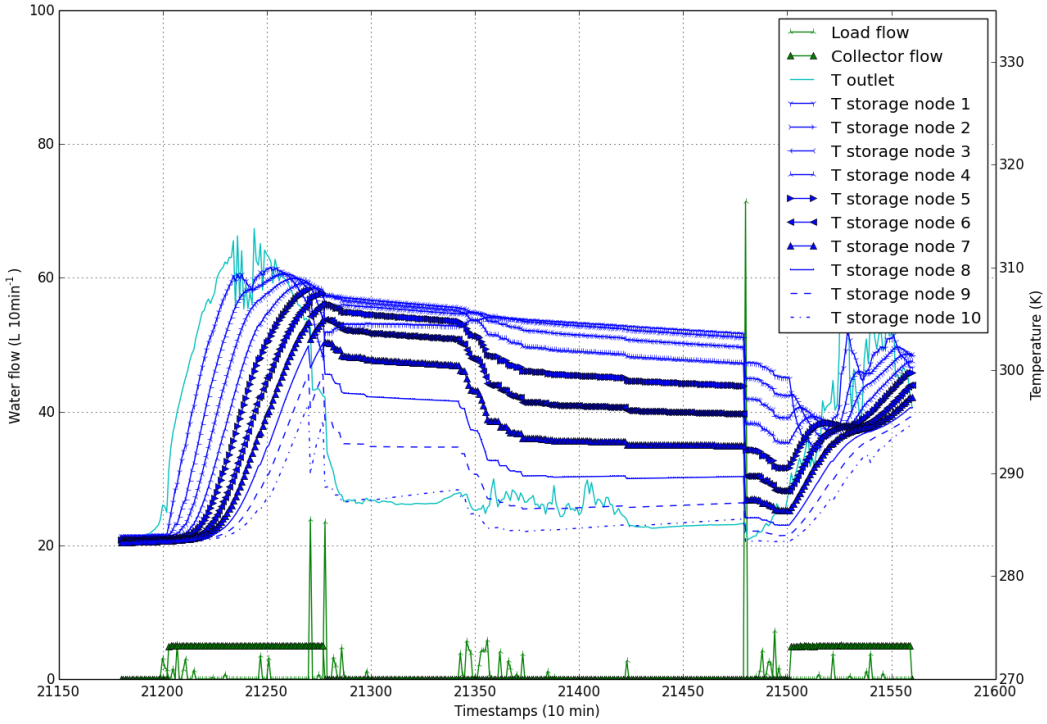

Table 9 shows the relations of stratification with storage temperatures and outputs.

Table 9 Level of stratification for different storage tanks and the influence on thermal efficiency

Level of stratification	4 nodes	10 nodes
Maximum upper storage tank temperature (K)	309.6	310.0
Maximum bottom storage tank temperature (K)	297.9	296.7
Average temperature difference between bottom and upper node (K)	11.8	15.5
Useful energy gain (MJ)	39.2	40.6
Electricity production (MJ)	10.9	11.1
Thermal efficiency	0.46	0.48
Electrical efficiency	0.129	0.130

4.3 Experimental validation

For the experimental validation, weather data with a one-minute resolution are used as input for the PVT model to reproduce the experimental output data. The prototype unglazed channel PVT collector with a surface of 0.34 m^2 is developed by DNV GL and the same company also does the measurements. Since a few parameters could not be determined in advance, they are estimated (see Table 6). The results of the first estimation are visualized in Figure 24.

Figure 24 Experimental results vs. first quess simulation results

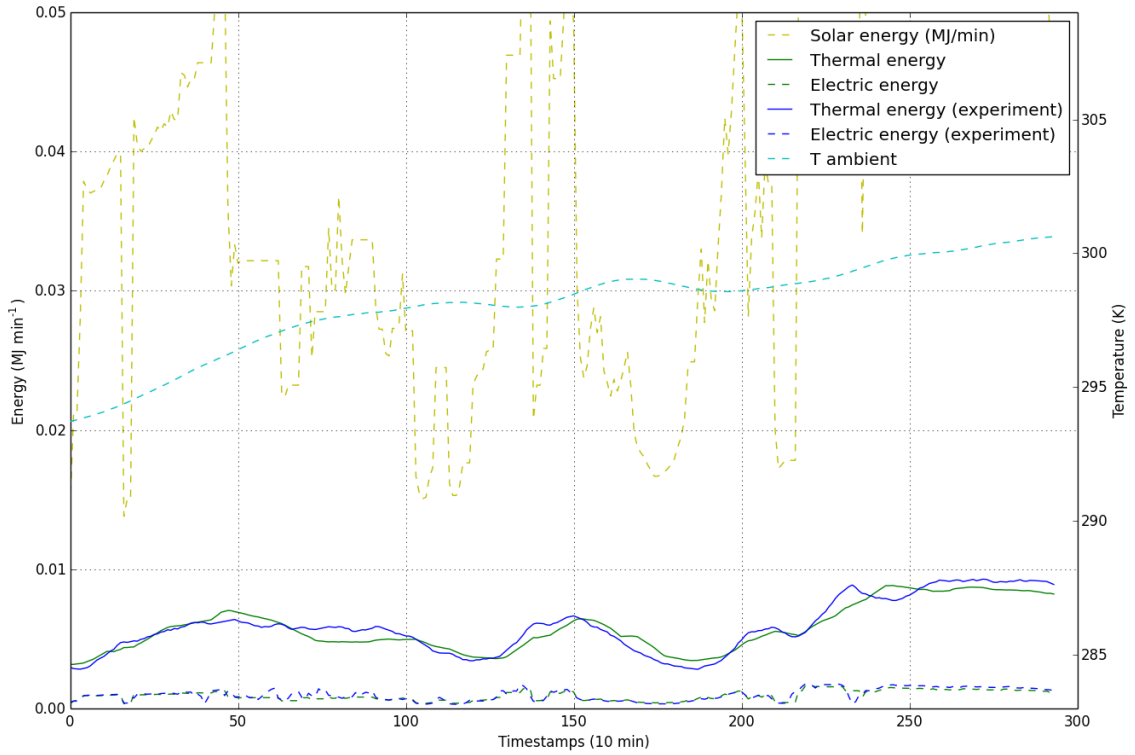

As explained in the methods, the uncertain parameters are optimised in a script using equations 37 and using equations 37 and 38. The results of this optimisation step are presented in Figure 25 (best root mean square percent deviation fit) and in

Table 10 the results are given for both the root mean square percent deviation and the correlation coefficient. In both cases the product of the thermal and electrical fit is used to determine the most optimal values for the parameters. Note that some parameters change significantly after the optimisation step.

Figure 25 Experimental results vs. optimised simulation results

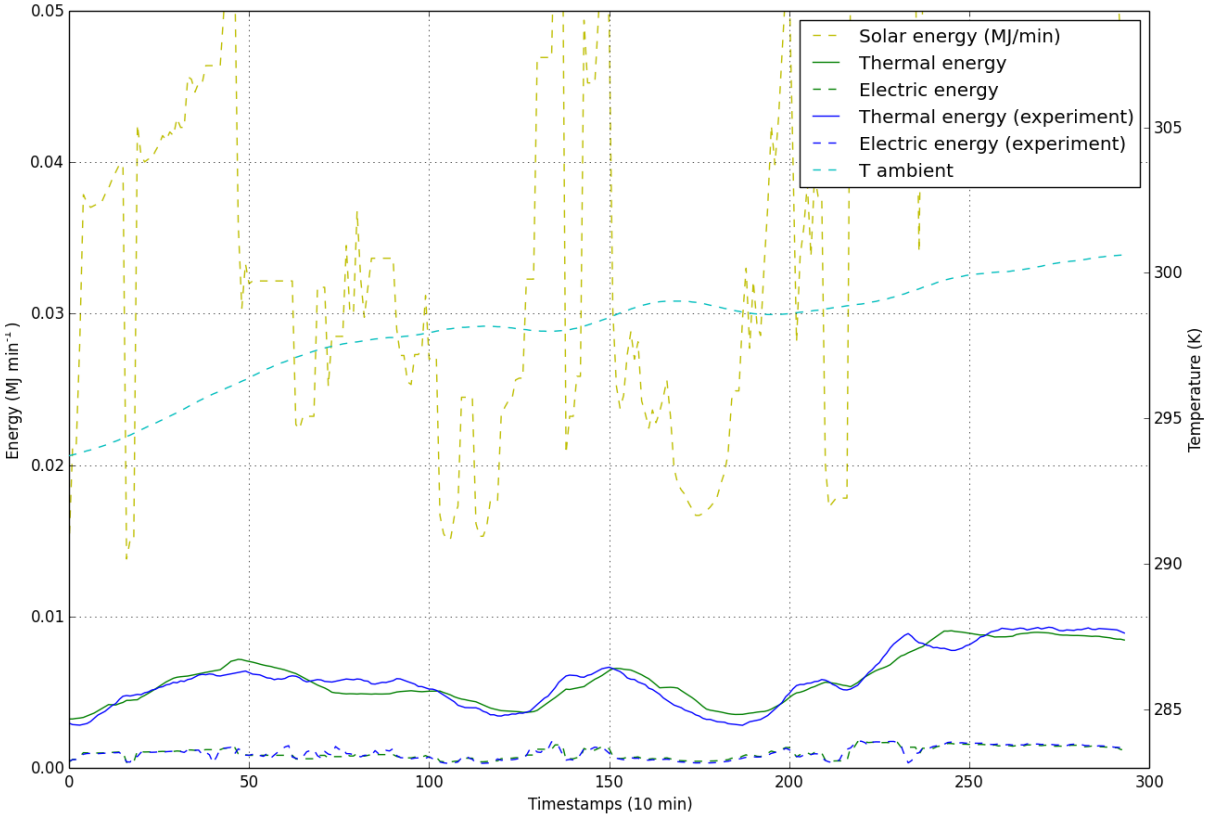

Table 10 Results of the r-fit and e-fit on the values of the parameters

Parameter/property/ result	**First guess**	**Best r-fit** (eq. 37)	**Best e-fit** (eq. 38)	**Unit**
PV reference efficiency	0.062	0.076	0.077	-
PV temperature coefficient	-0.002	-0.002	-0.002	K^{-1}
Heat transfer coefficient between cell and absorber	20	30	22.5	$W/(m^2*K)$
Plate emissivity	0.8	0.83	0.82	-
PV effective transmittance-absorption product	0.835	0.835	0.835	-
Conduction insulation	0.033	0.0445	0.0445	W/(m*K)
Bond thermal conduction	0.2	0.5	0.5	W/(m*K)

Difference in heat production model and measured	-1.7	6.8	0.28	%
Difference in electricity production model and measured	-20.0	-1.1	-0.16	%

4.4 Optimisation of a PVT collector

The optimisation procedure is explained in the methods and is performed for glazed and unglazed channel PVT collectors. In this optimisation step, first the tube diameter and the plate to cover distance is optimised for a glazed channel and unglazed channel PVT collector. The optimisation step showed that for the glazed channel PVT collector a tube diameter of 0.003 m in combination with a plate-cover distance of 0.034 m resulted in the lowest simple payback period. For the unglazed channel PVT collector, a tube diameter of 0.004 m is optimal. The costs for this optimisation are presented in Table 7 and the initial choices for all other parameters in Table 4.

The second optimization step is performed based on different PV cells, different channels, differing flow rates and pump control schemes. The different materials and the associated costs and exergy are presented in Table 11 for all systems with an optimised flow rate and pump control scheme.

Table 11 Results of the optimisation step

Type	Channel material	PV type	Exergy (MJ)	PBP (year)	Investment costs (€)	Gas savings (€/year)	Net electricity benefits (€/year)
Glazed	Copper	c-Si PUM	806	14.7	1276	41.15	45.57
		c-Si EWT	869	14.2	1297	41.84	49.21
		a-Si	464	17.1	1124	40.91	24.82
		CIGS	657	14.8	1188	44.63	35.79
	HDPE	c-Si PUM	807	14.6	1265	40.89	45.61
		c-Si EWT	***869***	***14.2***	***1286***	***41.59***	***49.26***
		a-Si	464	17.0	1113	40.65	24.83
		CIGS	656	14.7	1178	44.44	35.82
Unglazed	Copper	c-Si PUM	808	15.5	1161	27.46	47.65
		c-Si EWT	870	14.9	1181	27.78	51.41
		a-Si	460	18.7	1009	27.49	26.52
		CIGS	649	16.0	1073	29.30	37.77
	HDPE	c-Si PUM	808	15.4	1150	27.21	47.67
		c-Si EWT	***870***	***14.8***	***1172***	***27.53***	***51.43***
		a-Si	459	18.6	998	27.25	26.53
		CIGS	648	15.9	1063	29.04	37.78

In each optimisation step, the smallest T_{off} and T_{on} (1 and 4 K respectively) resulted in the highest exergy and lowest payback period. The most efficient PV cell is in both cases the c-Si EWT panel and for both collector types the HDPE channel resulted lower payback periods. A sensitivity analysis is shown in Figure 26 where the influence of the flow rate on the exergy and payback period is visualised for the c-Si EWT glazed and unglazed HDPE channel collectors. This graph also shows that the optimum flow rate is comparable for both PVT collectors and is optimal around 0.003-0.004 kg/(s*m^2). The annual thermal efficiency of the optimized glazed and unglazed PVT collector are 0.42 and 0.28 respectively.

Figure 26 The exergy and PBP as a function of flow rate

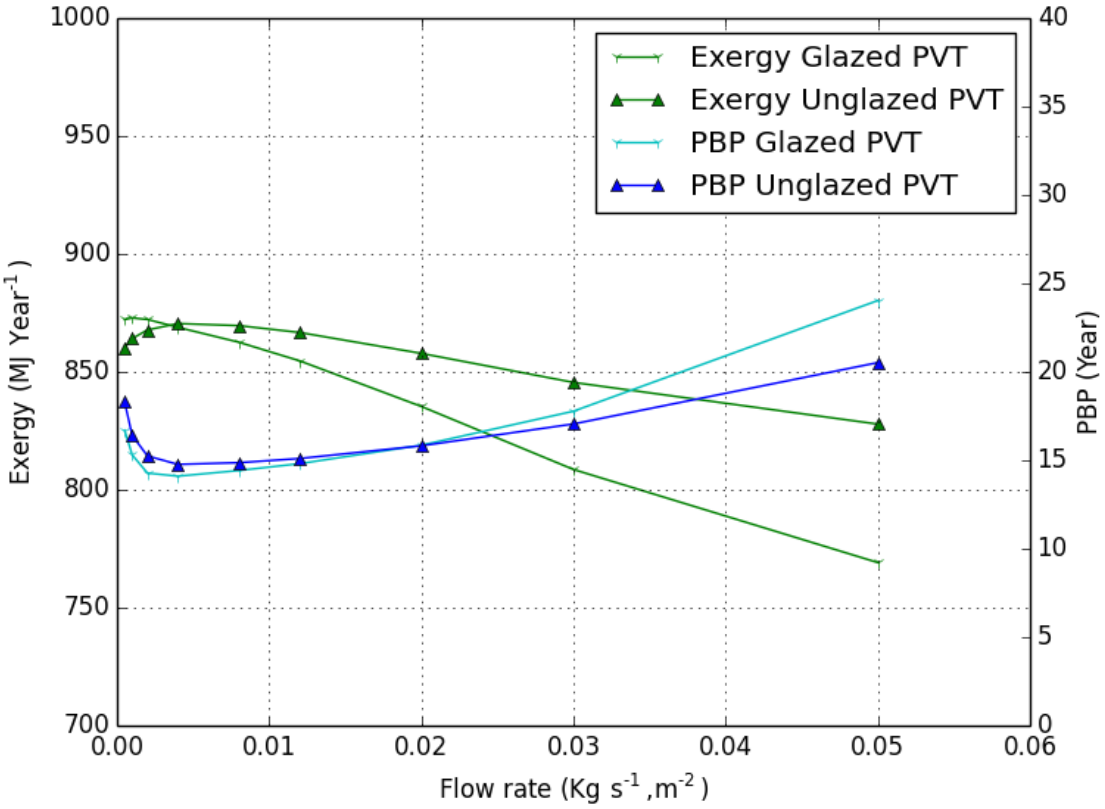

4.4 Optimisation of the total PVT system

The optimization of the total system is based on three different PVT collectors; the prototype, the optimized glazed PVT collector and the optimized unglazed PVT collector. Since the costs of the prototype is difficult to determine, it is assumed that the costs are identical to that of the unglazed PVT collector with instead of a-Si PV, a solar panel produced by Hyet Solar (around 2.00 €/W_p). Similar as in the methods, the results are presented for all three system configurations.

Preheating DHW

In this system several dimensioning and capacity parameters are evaluated and optimised as explained in the methods. In all cases, the storage tank modelled with 10 nodes resulted in lower payback periods due to higher levels of stratification. The smallest T_{off} and T_{on} that are analysed in the model (1 and 4 K respectively) resulted in the lowest payback period. Figure 27 shows the influence of storage tank size and collector area of an optimised glazed PVT collector on the payback period, maximum storage temperature, gas savings, electricity savings and the error as defined by equation 25. All steps have been optimised for the flow rate, which is also shown in the figure.

Figure 27 Influence of storage size and collector area on different outputs

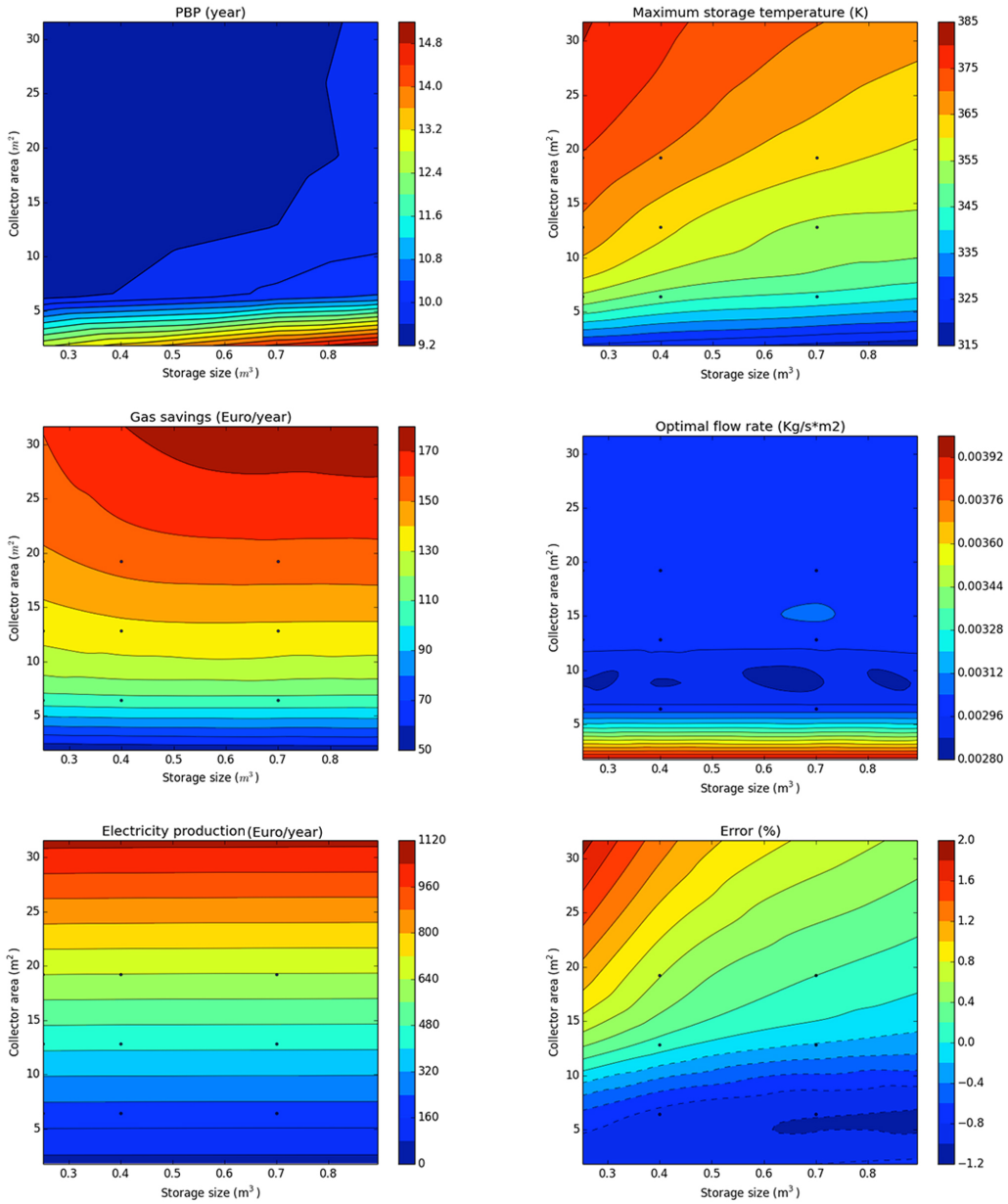

The same results are presented for the optimised unglazed PVT collector in Figure 28.

Figure 28 Influence of storage size and collector area on different outputs

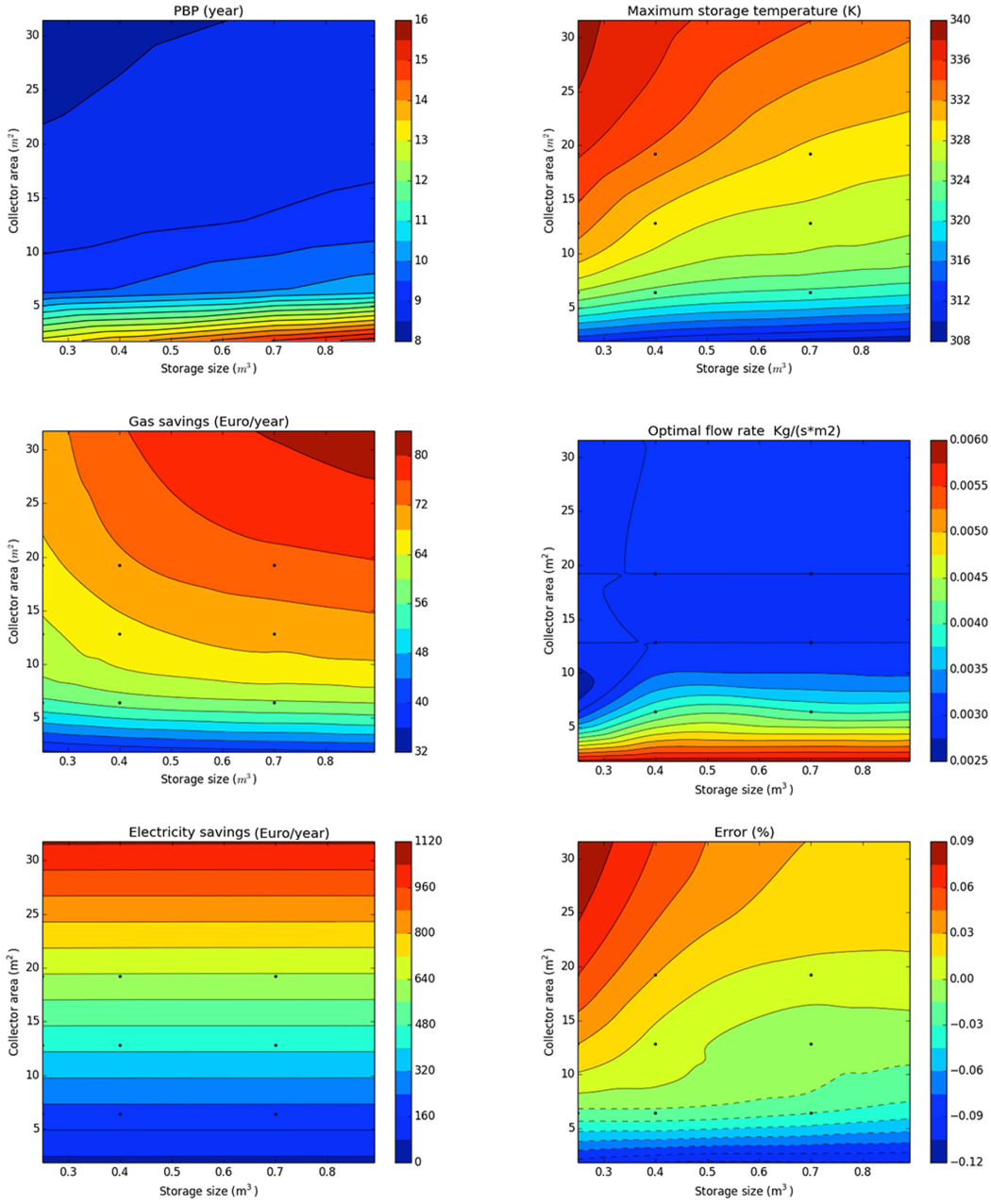

The outcomes of all DHW system optimisations for the optimised glazed PVT collector, the optimised unglazed PVT collector and the unglazed prototype PVT collector are presented in Table 12. The results are presented for three different household types.

Table 12 Optimised values and results for different PVT systems and households for preheating water for DHW

Collector type	Household type	Area (m^2)	Storage tank size (m^3)	PBP (years)	Installation costs (€)	Investment costs (€)	Gas savings (€/year)	Electricity benefits (€/year)	Optimal flow rate (kg/(m^2*s))
Glazed PVT	Large	11.2	0.211	9.2	850	3698	126	367	0.003
	Medium	16.0	0.222	9.6	1000	5211	113	534	0.003
	Small	33.6	0.236	9.9	1550	10743	94	984	0.003
Unglazed PVT	Large	34.4	0.216	8.4	1575	8524	68	1137	0.003
	Medium	34.1	0.230	8.5	1565	8454	55	1127	0.003
	Small	34.7	0.228	8.5	1585	8609	42	1151	0.003
Unglazed PVT prototype	Large	28.8	0.283	14.5	1400	6619	73	478	0.003
	Medium	14.9	0.244	14.9	1000	3755	53	266	0.003
	Small	14.4	0.179	15.5	950	3362	39	239	0.003

The most optimal system is for an unglazed optimised PVT system applied in a large household. In Figure 29 the volume and flow rate are fixed at the optimised level and the collector area is varied for a large household to see the influence of the area on the PBP for optimised glazed and unglazed PVT collectors. Note that the optimum PBP for unglazed PVT collectors stabilizes around 34.4 m^2.

Figure 29 The influence of area on PBP

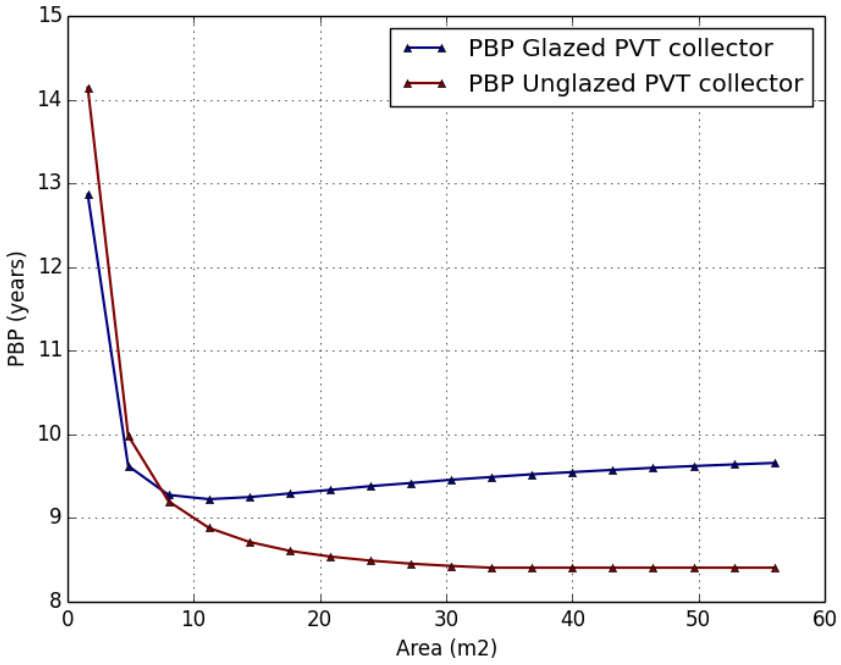

Figure 30 displays a sensitivity analysis for both unglazed and glazed optimised PVT collectors where the storage tank volume is varied at the optimum conditions that are shown in Table 12.

Figure 30 The influence of storage tank size on PBP

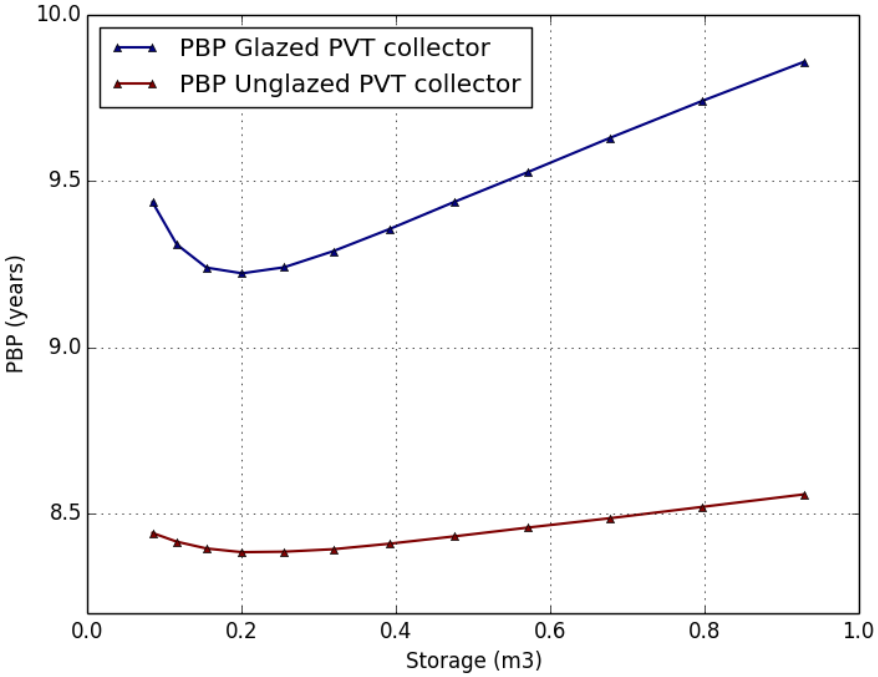

Preheater heat pump for low temperature space heating

In this system several dimensioning, capacity and other parameters are evaluated and optimised as explained in the methods. In all cases, the storage tank modelled with 10 nodes resulted in lower payback periods due to higher levels of stratification. Again also the smallest T_{off} and T_{on} that are analysed in the model (1 and 4 K respectively) resulted in the lowest payback period in every case. The results are shown in Table 13. Note that the reference heat pump system has the same capacity as the one used in the PVT system and this capacity is determined as share of the maximum heat demand.

Table 13 Optimised values and results for different PVT systems and households for preheating water for low temperature central heating

Collector type	**Household type**	**Area** (m^2)	**Storage tank size** (m^3)	**PBP** (years)	**Installation costs** (€)	**Investment costs** (€)	**Gas savings** (€/year)	**Electricity benefits-costs*** (€/year)	**Optimal flow rate** ($kg/(m^{2*}s)$)
Glazed PVT	Large	33.6	0.571	16.1	1550	20126	489	856	0.0075

	Medium	32	0.432	16.4	1500	19503	365	912	0.0075
	Small	32	0.392	17.0	1500	19369	267	961	0.007
Unglazed PVT	Large	33.6	0.476	17.4	1550	20490	321	943	0.0065
	Medium	33.6	0.467	17.4	1550	20361	257	985	0.0065
	Small	33.6	0.433	18.0	1500	20167	178	1030	0.0065
Unglazed PVT prototype	Large	67.2	0.677	25.3	2600	30348	397	903	0.004
	Medium	64	0.612	25.7	2500	29148	317	912	0.004
	Small	64	0.570	26.5	2500	28984	212	976	0.004
	Household type	**Heat pump capacity** (kW)	**Average COP**	**Average COP heat pump ref.**	**Investment costs heat pump ref** (€)	**Minimum allowable storage temperature** (°C)	**Total heat output heat pump** (GJ)	**Total heat output heat pump reference** (GJ)	**Additional gas input** (GJ)
Glazed PVT	Large	2.09	5.9	3.9	24054	285	27	70	129
	Medium	2.07	6.0	3.8	23865	285	21	35	51
	Small	1.98	5.3	3.4	23100	285	15	27	33
Unglazed PVT	Large	2.40	5.6	4.7	26776	281	18	106	138
	Medium	2.31	5.5	4.6	26073	281	14	48	57
	Small	2.17	5.2	4.2	24756	280	9.3	36	39
Unglazed PVT prototype	Large	2.40	5.7	4.7	26776	280	22	106	134
	Medium	2.27	5.5	4.5	25600	280	17	47	54
	Small	2.16	5.3	4.2	24628	280	12	36	36
* When costs exceed benefits, value is presented with a minus sign									

In Figure 33 the flow rate and volume rate are fixed at the optimised level and the collector area is varied for a large household to see the influence of the area on the PBP for optimised glazed and unglazed PVT collectors.

Figure 31 The influence of area on PBP

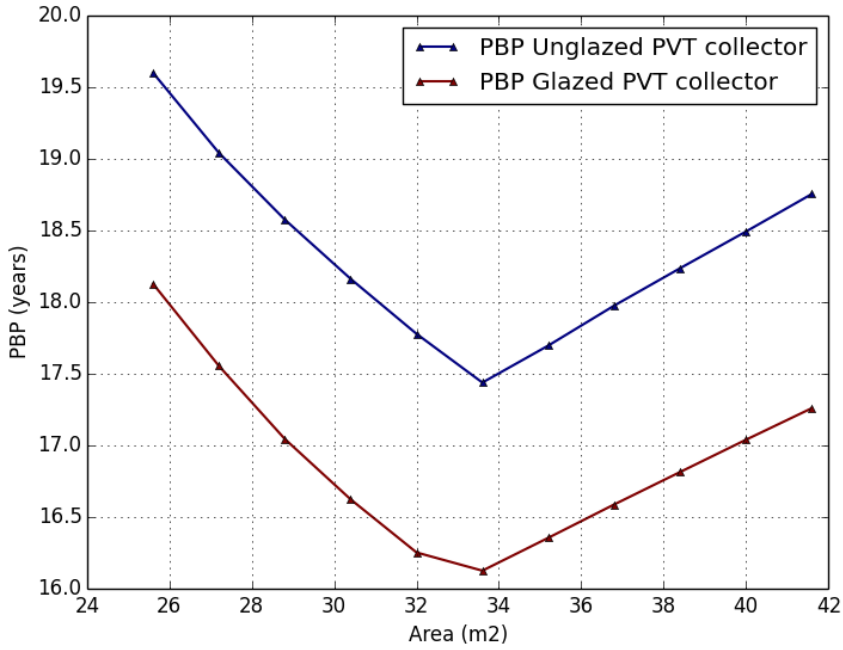

In Figure 33 the flow rate and area are fixed at the optimised level and now the varied parameter is the volume of the storage tank. This situation is also for a large household and for optimised glazed and unglazed PVT collectors.

Figure 32 The influence of storage tank size on PBP

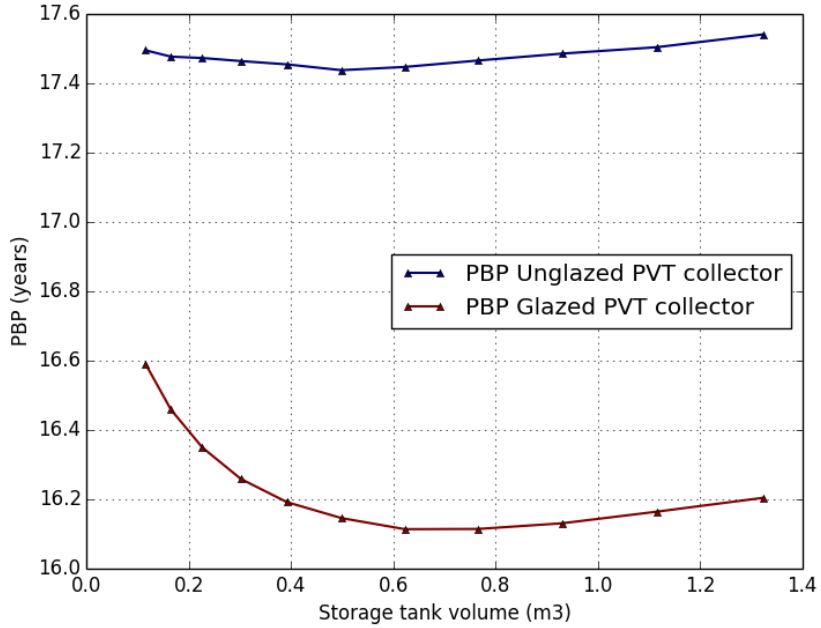

Preheater for DHW and heat pump for low temperature space heating

In this system two storage tanks are used; one for preheating DHW and the other larger tank for preheating water for the heat pump. As the computing time for this system is significantly larger than for the other systems, it is chosen to only present the results for large households. As explained in the methods, the collector flow can be switched between the two storage tanks based on a control scheme. By default the collector flow uses water from the heat pump storage tank unless the storage tank temperature exceeds the temperature of the water leaving the heat pump or if the outlet temperature of the PVT collector exceeds a certain threshold. This threshold is one objective of the optimisation step. Others are the optimal flow rate, collector area, storage tank size of the heat pump (for simplicity, the storage tank for DHW is fixed at 500 L), capacity of the heat pump and the minimum required storage temperature for the operation of the heat pump. The results are shown in Table 14.

Table 14 Optimised values and results for different PVT systems and households for preheating water for DHW and low temperature central heating

Collector type	**Household type**	**Area** (m^2)	**Storage tank size** (m^3)	**PBP** (years)	**Installation costs** (€)	**Investment costs** (€)	**Gas savings*** (€/year)	**Electricity benefits-costs**** (€/year)	**Optimal flow rate** (kg/(m^2*s))
Glazed PVT	Large	33.6	0.569	15.8	1550	20408	408 130	851	0.007
Unglazed PVT	Large	33.6	0.318	17.1	1550	20667	279 51	965	0.006
Unglazed PVT prototype	Large	67.2	1.076	24.8	2600	30791	334 64	949	0.004
	Household type	**Heat pump capacity** (kW)	**Average COP**	**Average COP heat pump ref.**	**Investment costs heat pump ref** (€)	**Minimum allowable storage temperature** (°C)	**Total heat output heat pump** (GJ)	**Total heat output heat pump reference** (GJ)	**Additional gas input***** (GJ)
Glazed PVT	Large	2.07	5.9	3.9	23860	285	23	67	133
Unglazed PVT	Large	2.36	5.5	4.7	26387	281	16	102	140

Unglazed PVT prototype	Large	2.38	5.8	4.7	26582	281	19	104	137

* Gas savings include two numbers; the first is for gas savings concerning low temperature central heating, and the second for gas savings associated with the preheated water for DHW

** When costs exceed benefits, value is presented with a minus sign

*** This only includes the gas input for additional low temperature central heating

5 Discussion

The discussion will be split up according to the different subjects presented in the previous chapter. After discussing the results some uncertainties will be examined.

PVT model

Figure 18 shows the thermal efficiency curves for different designs: channel, sheet-tube, glazed and unglazed. In this figure, identical conditions have been used to that of the reference scenario for a fair comparison. Both the glazed and unglazed PVT collectors show almost identical thermal efficiency curves compared to the reference, which is also simulated using a 1D simulation model based on the Hottel and Whillier equations. The only difference is that the reference curve decreases somewhat faster indicating a higher overall loss coefficient (eq 11) since this coefficient is the largest determinant of a lower thermal efficiency at high differences between T_{inlet} and T_{amb}. One reason could be that the overall loss coefficient in the study of Zondag et al is calculated in a different way; they use a empirical relation between several weather conditions, parameters and the overall loss coefficient (Zondag H. , de Vries, van Helden, van Zolingen, & van Steenhoven, 2003).

In Figure 20 the efficiency curves are displayed for PVT collectors where the PVT parts are eliminated per curve that results in a transformation of the PVT collector into a standard flat plate solar thermal collector. When the most upper curve is compared with a reference flat plate solar thermal collector as shown in Figure 33, it can be seen that this statement is supported by the results.

Figure 33 Efficiency curve comparison with reference

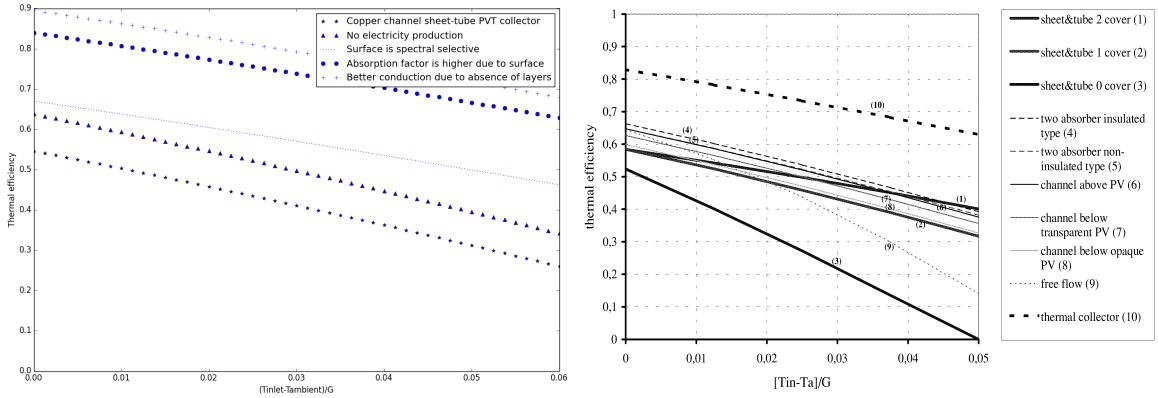

Storage tank model

The simulation of the storage tank is done in 10 nodes, which is most accurate according to literature as mentioned earlier. According to Newton, the DIFFEQ integration method performs better in terms of a smaller error (as defined by eq 25). The results in presented in Table 8 confirm this statement and therefore the DIFFEQ

integration method is used for all simulations where a storage tank is used. Also the claim that modelling in more nodes will result in higher stratification is confirmed by Table 9 and it is also shown that more stratification leads to higher thermal yields.

Experimental validation

In this section the experimental results with a one-minute resolution of five hours is simulated with the PVT model. First the parameters have been estimated and as Figure 24 and Table show, the results of the simulation model are already quite close to the experimental ones. After an optimisation step where all uncertain parameters have been optimised for a better fit, the error is reduced significantly and the difference in heat and electricity production as simulated by the PVT model differs only 0.28 % and -0.16 % respectively.

Unfortunately it was only possible to compare simulated results with experimental results for one day of measurements. More measurements are performed by DNV GL but in these measurements the flow rate is changed during the experiment to uncertain values and could thus not be compared.

Still there are some deviations between experimental and simulated values. For the thermal part this could possibly be explained by the fact that the simulated results are based on a steady state model. This means that output equals input, and although T_{inlet} is taken from a timestep one circulation time period before the evaluated timestep where T_{outlet} is determined, this stays an assumption. It very unlikely that exactly the same water molecules entering the PVT collector will leave the PVT collector exactly after the circulation time. This is mainly caused by processes such as turbulence and since the water in the prototype faces a lot of resistance by corners in the tubing system, the exact location of the water is very hard to determine and beyond the scope of this research.

The differences between the electrical output experimentally and simulated are possibly due to the following reason; the weather conditions such as solar radiation are measured every minute in contrast to the electrical output that is measured with a cumulative measurement device. This results in possible errors in the simulation model since for example some clouds are not included in the weather data, which act as input for the PVT model, whereas the clouds are incorporated in the measured electrical output. Since the thermal model uses the circulation time averaged weather conditions as input, these errors have a significant smaller influence on the thermal results than the electrical results.

Optimization of a PVT collector

For the optimization of the PVT collector, a system is of one collector (area 1.6 m^2) is chosen in combination with a heat exchanger effectiveness of 0.9 and a storage tank of 300 L. This system is simulated using a large consumer DHW load profile and a condensing boiler of 59 kW is used, as this capacity is large enough to cover the maximum DHW demand. For both the glazed and unglazed PVT collector the c-Si EWT PV cell performs best since this resulted in higher electrical yields in

combination with large gas savings. Although the CIGS PV cell has larger gas savings, this does not compensate the loss in electric efficiency. Also the HDPE tubing system resulted in lower investment costs than the copper tubing system for both the glazed and unglazed PVT collector. Still this system needs to be evaluated experimentally since high temperatures could lead to thermal expansion and thereby jeopardize the stability of the PVT collector. These same conclusions also hold for the total exergy of the system and this result strengthens the choice for the c-Si EWT PVT collector.

It is remarkable that the optimal flow rate is so much lower than normally used in literature for simulations, which is around 0.02 kg/(s*m^2) (Zondag H. , 2008). This value is also used mostly for flat plate solar thermal collectors but since the associated temperatures are much higher than for PVT collectors it makes sense that the flow rate has to be decreased for PVT collectors. This is mainly due to the operation of the pump since a certain temperature difference between the storage tank and the collector outlet is required. Although the thermal efficiency of the PVT collector increases at higher flow rates, the consequence is that the operation time of the pump drops significantly. Also the pump control scheme is much lower than for flat plate solar thermal collectors; a T_{off} and T_{on} of 1 and 4 K respectively is optimal for PVT collectors as for flat plate solar thermal collectors this is 4 K and 8 K respectively. An additional effect of a larger operation time of the pump is that the PV cells are more often cooled increasing the electric yield.

The annual thermal efficiency of the optimized glazed and unglazed PVT collector are 0.42 and 0.28 respectively and this is higher than reference values as reported by Zondag et al which are 0.35 and 0.24 respectively (Zondag & van Helden, 2003). Probably this is the result of a higher flow rate and a higher required temperature difference for pump operation since the reference system is not optimised for these two parameters.

Optimization of the total PVT system

Preheating DHW

The first graph in Figure 27 shows the PBP as a function of collector area and storage tank size for a glazed PVT collector applied for preheating DHW in a large household. Since a larger collector area results in higher electrical yields, which outweigh the savings in gas, the PBP is lowest at large collector areas. Although a lower storage tank size results in somewhat lower gas savings, the associated reduction in investment costs leads to a lower PBP. Figure 27 also shows that systems with lower collector area perform better with a slightly higher flow rate than large collector area systems. Also it is shown that the error becomes larger when the collector area increases with respect to storage tank volume and this is caused by the numerical integration method that is used for the simulation of the storage tank. One important note that this research does not consider is the maximum allowable operation temperature of the water. As shown, with large collector area and small storage tanks this temperature could exceed 100 °C with potentially could damage the PVT collector and though the working fluid contains a water/ethylene glycol

mixture increasing the boiling temperature, it could still be that the water must be pressurized in order to avoid vapor formation.

For the unglazed PVT collector the results are comparable with the results for glazed PVT collectors. Still it must be noted that unglazed reactors have higher electrical yields due to the absence of a glass cover, which results in additional cooling of the PV cell, less transmission losses and lower plate temperatures. This given also results in less gas savings but as Table 12 the optimal unglazed PVT collector has a lower PBP indicating that the gains in electric yield and lower investment costs outweigh the loss in gas savings. The PBP of the unglazed PVT collector for a large household is around 8.4 years as for the optimised glazed PVT collector this is 9.2 years.

The PBP of the prototype is much larger than the optimised systems mainly due to a significant loss in electric yield due to the Hyet Solar PV cells that are almost two times less efficient. The gas savings are higher than the optimised unglazed PVT collector due to lower electric yields resulting in more residual solar energy that can be utilized for heat production, still this has only a marginal effect on the PBP.

The sensitivity analysis presented in Figure 29 shows that an increasing collector area after the optimum level results in an increasing PBP, which is not the case for unglazed PVT collectors. This is due to the relatively higher investment costs associated with increased collector area. This effect does not occur for unglazed PVT collectors.

The sensitivity analysis in Figure 30 shows a steeper increase in PBP after the optimum level for glazed PVT collectors than for unglazed PVT collectors. This is due to the fact that the investment costs associated with the storage tank play a larger role in the PBP for glazed PVT collectors since the overall investment costs are lower due to a lower optimal collector area.

Preheater heat pump for low temperature space heating

In Table 13 all results are presented concerning the optimised PVT systems for different households. In this case the optimised glazed PVT collector outperforms the optimised unglazed PVT collector (PBP of 16.1 years vs. 17.4 years). As in this system the electricity price reduces after producing more than 5000 kWh, almost all PBPs of optimised PVT collectors are within the range of 32-33.6 m^2. This observation is also confirmed by the sensitivity analysis shown in Figure 33. If more PVT collectors are added, the electricity benefits reduce significantly as the 5000 kWh boundary is crossed.

As expected, in all cases the operation time of the heat pump is significantly smaller than the reference heat pump system since the operation has to meet certain requirements to avoid the storage tank being depleted. Further more it is shown that the optimal heat pump capacity is relatively (with respect to total heat demand) higher for small households than for large households and the percentage of total heat that is covered by the heat pump is 0.17, 0.29 and 0.31 for large, medium and

small households respectively. The COP is closely related with the heat pump capacity and the optimal pump flow rate is related to the heat producing capacity of the PVT collector and thus lower for unglazed PVT collectors. The electric benefits are higher for smaller households than for large ones. This is not because of higher electricity production but the result of a lower heat demand that leads to less use of the heat pump and thus lower electricity costs.

Again the prototype performs worse than the optimised PVT collectors. This is mainly due to higher investment costs associated with a higher collector area that is required due to less electric yield. Note however that the reference heat pump has the same capacity as the heat pump used in the PVT system, which leads to a false comparison since the reference heat pump is not optimised in this way. Unfortunately results could not be compared with references since no literature is found that reports about the same system configuration.

Preheater for DHW and heat pump for low temperature space heating

Table 14 shows all results from the optimisation procedure for this PVT system. The best performing PVT collector is again the optimised glazed collector with a PBP of 15.8 years. However this system has a somewhat lower PBP than in the previous examined PVT system, it must be noted that the benefits of gas savings are rather small compared to the total amount of costs and benefits. This means that the DHW part of this system has a marginal influence on the result and much of the same conclusions can be drawn for this system as for the previous system. One observation that is typical for this system is that the required outlet temperature that switches the pump from load the heat pump storage tank to loading the DHW storage tank differs between the different systems. This is because the glazed PVT collector achieves higher temperatures more frequently and thus a higher temperature difference is optimal.

Uncertainties

Uncertainties in the modeling aspect are mainly a result of all the different assumptions that had to be made to develop a one-dimensional simulation model. Aside from the assumptions listed in section 2.6.2 other effects have been neglected in the model; the heat capacity of the PVT system and the effect of rain on the annual yield. Also some empirical equations are used in the report, such as determining the sky temperature and determining the convection as a function of wind speed, and these relations have not been experimentally tested in this report. Additionally the PVT model uses average 10-minute weather data and the model only evaluates one year, which results in a less trustworthy payback time period. Also the stability of the PVT system is not simulated resulting in less reliable optimization results.

The optimization procedure as explained in the methods is also a source of potential uncertainties since the optimization procedure assumes absolute minima and could trap in local minima concerning the payback period. To avoid trapping into local minima, the optimization procedure is repeated with different start values for the

parameters but still it cannot be excluded with certainty. As the model for the PVT collector is been validated by experimental data, this is not the case for the other modeled components like the storage tank, heat exchanger, auxiliary boiler, heat pump, circulation pump and the piping system. This is an additional source of potential errors.

For the calculation of the simple payback period, a lot of assumption had to be made concerning the costs of different materials and components. Also the limited availability of literature for the evaluation of the influence of capacity and size on costs have contributed to less reliable results. Especially the heat pump investment costs are difficult to examine since these costs differ significantly between households. This is due to the differences in local conditions, like the difficulties installing a closed or open loop system for a heat pump, which have a large influence on the investment costs. Also the installation costs of the PVT system are hard to examine since these costs are not known and are now estimated using installation costs of PV and flat plate solar thermal collectors.

6 Conclusions

In this report glazed and unglazed PVT collectors are examined and research is conducted to find the most optimal heat application for different household sizes. Firstly, a one-dimensional model is developed that is able to simulate different types of PVT collectors. Secondly, this system is dynamically coupled to different heat utilization options and all required components like a heat exchanger, storage tank and auxiliary boiler are simulated individually. Thirdly, all the sizes and materials used in the different components are linked to cost functions and all energy savings/costs are linked to prices enabling the model to evaluate and optimise the system based on the simple payback period.

A prototype unglazed PVT collector is developed within the Nanosol project and tested experimentally and the simulation model is validated by the experimental results. The simulations make use of a thermal model based on the equations of Hottel and Whillier. After the validation, the glazed and unglazed PVT collectors are optimised for different PV types, tubing materials, dimensions, flow rate and other parameters. For both glazed as unglazed it is shown that the PV c-Si EWT PV cell in combination with a HDPE tubing system results in the lowest payback period. This is because c-Si EWT PV cells have high electric efficiencies and the electric savings outweigh the gas savings that are a result of the produced heat. Also it is shown that a low required temperature difference between the outlet water and the bottom of the storage tank resulted in higher operation times of the circulation pump and thereby increasing the annual yield of the PVT collectors. Additionally a low flow rate resulted in higher outlet temperatures further increasing the operation time of the circulation pump.

Literature has pointed out that three systems are promising for utilizing the heat produced by PVT collectors since the reached temperatures are lower than for flat plate solar thermal collectors; preheating water for DHW, preheating water for a heat pump and a combination of both. All these systems are optimised and use the optimised glazed PVT collector, optimised unglazed PVT collector and prototype PVT collector as a heat source. Results show that the lowest simple payback period is for using an unglazed PVT collector applied for preheating DHW for a large household. The optimised simple payback period for this PVT system is 8.4 years and mainly the electric yield is decisive for this result. This optimised system has a collector area of 34.4 m^2 and a storage tank volume of 216 L that is modelled with 10 nodes to increase the stratification in the tank.

Another observation is that a small flow rate is often optimal since this leads to higher PVT outlet temperatures resulting in a higher operation time of the circulation pump. Aside from the associated gas savings, a higher operation time also results in more cooling which increases the electrical yield of the PV cells. Also the results show that the production of electricity is decisive for both the exergy and the simple payback period.

Using PVT collectors for preheating water in a heat pump is less beneficial and the lowest payback period is achieved by a glazed PVT collector (16.4 years). A combination of both systems led to comparable results to the PVT heat pump system. Still the additional functionality enabling the system to also load the DHW storage tank, reduced the simple payback period slightly to 15.8 years.

For further research it is recommended to experimentally validate the results for the different components such as the storage tank, auxiliary boiler, heat pump and heat exchanger. Also it is recommended to have a more precise estimation of all costs associated with the different systems and to evaluate more different types of household as the results show that the payback period is very dependent on the size and type of the household. Further it is recommended to evaluate the payback period using different yearly weather datasets.

7 Appendix

A Curve fitted equations

Air properties:

$$k_{air} = 7E^{-5} * T_{air} + 0.0052$$
$$\alpha_{air} = T_{air} * 1.484E^{-7} - 2.23E^{-5}$$
$$\nu_{water} = 1.01E^{-7} * T_{fluid} - 1.46E^{-4}$$

Water properties:

$$k_{water} = -9.5E^{-6} * T_{fluid}^2 + 0.0073 * T_{fluid} - 0.724$$
$$\alpha_{water} = 3.4E^{-10} * T_{fluid} + 4.1E^{-8}$$
$$\nu_{air} = 2.3E^{7} * T_{fluid}^{-5.42}$$
$$C_{p-water} = 0.0121 * T_{fluid}^2 - 7.64 * T_{fluid} + 5385.2$$
$$\rho_{water} = -0.0034 * T_{fluid}^2 + 1.77 * T_{fluid} + 771.8$$

Water/ethylene glycol mixture (40%):

$$k_{water} = -4E^{-7} * T_{fluid}^2 + 0.0031 * T_{fluid} - 0.172$$
$$\alpha_{water} = 1.8E^{-10} * T_{fluid} + 7.1E^{-8}$$
$$\nu_{water} = 7E^{13} * T_{fluid}^{-7.82}$$
$$C_{p-water} = 3.360 * T_{fluid} + 2484.2$$
$$\rho_{water} = -0.0024 * T_{fluid}^2 + 1.021 * T_{fluid} + 970.6$$

B Cost functions

Component	Equation	Remark/source
Epoxy storage tank with heat exchanger	$Investment(€) = 3.1087 * Volume(L)^{0.7417}$	(Rodríguez-Hidalgo, Rodríguez-Aumente , Lecuona, Legrand, & Ventas, 2012)
Water-to-water heat pump	$Investment(€) = 1307.1*\text{Capacity(kW)}+5842$	Based on Vaillant catalog data
Piping system	$Investment(€) = 75 + 10 * A_{pvt}$	Based on several solar collector tenders
PVT Installation costs	$Investment(€) = 500 + 50 * A_{pvt}$	(SMZ, 2013) and based on solar collector tenders
Inverter costs	$Investment(€) = -0.2*\ln(\text{DC input power(kW)})+0.656$	Cost function based on data provided by (SMZ, 2013)
Additional costs closed cycle (heat exchanger and installation costs)	$Investment(€) = 4500*\text{Capacity(kW)}$	(Warmtepomp informatie, 2013)
Additional costs open cycle (heat exchanger and installation costs)	$Investment(€) = 7400*\text{Capacity(kW)}$	(Warmtepomp informatie, 2013)

8 References

Assoa, Y., Menezo, C., Yezou, R., Fraisse, G., & Lefebvre, T. (2005). Passive and Low Energy Cooling for the Built Environment. *Study of a new concept of photovoltaic-thermal hybric collector*, (pp. 1-6). Santorini, Greece.

Bakker, M., Zondag, H., Elswijk, M., Strootman, K., & Jong, M. (2004). Performance and costs of a roof-sized PV/thermal array combined with a ground coupled heat pump. *Solar Energy* (78), 331-339.

Blok, K. (2007). Introduction to energy analysis. Utrecht: Techne Press.

Charalambous, P., Maidment , G., Kalogirou, S., & Yiakoumetti , K. (2007). Photovoltaic thermal (PV/T) collectors: A review . *Applied Thermal Engineering , 27*, 275-286.

Chow, T. (2010). A review on photovoltaic/thermal hybrid solar technology. *87*.

Chow, T. (2003). Performance analysis of photovoltaic-thermal collector by explicit dynamic model . *Solar Energy , 75*, 143-152.

Cristofari, C. N. (2003). Influence of the flow rate and the tank stratification degree on the performances of a solar flat-plate collector. . *International Journal of Thermal Sciences , 42*, 455–469 .

Cruickshank, C. A. (2009). PhD Thesis: Evaluation of a stratified multi-tank thermal storage for solar heating applications . In C. A. Cruickshank. Kingston, Canada: Queen's University .

de Vries, D. (1998). PhD Thesis: Design of a photovoltaic/thermal combi-panel. In D. W. de Vries. Eindhoven: Eindhoven University Press.

DTU. (2010). *Investigations on small low flow SDHW systems with different solar pumps and solar collector loops* . UK: DTU .

Duffie, J., & Beckman, W. (1991). Solar Engineering of Thermal Processes . New York: John Wiley & Sons Inc.

Duffie, J., & Beckman, W. (2013). Solar Engineering of Thermal Processes . John Wiley and Sons.

ECN. (2005). A roadmap for the development and market introduction of PVT technology. Bad Staffelstein, Germany: ECN.

ECN. (2005). PVT Roadmap: a European guide for the development and market introduction of PVT technology. (pp. 6-10). Barcelona, Spain : ECN.

EERE. (2013). *About EnergyPlus*. (EERE, Producer) Retrieved June Monday, 2014 from EnergyPlus Energy Simulation Software : http://apps1.eere.energy.gov/buildings/energyplus/energyplus_about.cfm

EnergyPlus. (2013). *EnergyPlus.* Retrieved June 23, 2014 from Input output reference document: http://apps1.eere.energy.gov/buildings/energyplus/pdfs/inputoutputreference.pdf

Garg , H., & Agarwal, R. (1994). Some aspects of a pv/t collector/forced circulation flat plate solar water heater with solar cells. *Eprint* , 1-16.

H.A. Zondag, de Vries, D., van Helden, W., van Zolingen, R., & van Steenhoven, A. (2003). The yield of different combined PV-thermal collector designs. *Solar Energy , 74*, 253-269.

Hottel, H., & Whillier, A. (1958). Evaluation of Flat-Plate Collector Performance. *Transactions of the Conference on the Use of Solar Energy , Vol. 2* (E. F. Carpenter, ed.), p. 74.

Hout & bouwmaterialen. (2011). *Prijslijst en leveringsprogramma*. Retrieved May 20, 2014 from Hout&bouwmaterialen.nl: http://www.hout-en-bouwmaterialen.nl/downloads/isobouw-prijslijst-en-leveringsprogramma.pdf

Houwing, M., Negenborn, R., & de Schutter, B. (2011). Demand Response With Micro-CHP Systems. *IEEE , Vol 99* (1), 200-211.

Huang, B., Lin, T., Hung , W., & Sun, F. (2001). Performance evaluation of solar photovoltaic/thermal systems. *Solar Energy , 70* (5), 443-448.

IEA. (2013). *Electricity/Heat in Netherlands in 2009*. Retrieved May 20, 2014 from http://www.iea.org/stats/electricitydata.asp?COUNTRY_CODE=NL

IPCC. (2007). *Climate Change: Synthesis Report.* International Panel on Climate Change. Geneva, Switzerland: IPCC.

IRENA. (2013). *Renewable energy technologies: Cost analysis series.* Solar photovoltaics . Bonn, Germany: IRENA.

Ji , J., Chow, T., & He, W. (2003). Dynamic performance of hybrid photovoltaic/thermal collector wall in Hong Kong. . *Building Environ* (38), 1327-34.

Jordan , U., & Vajen , K. (2005). DHWcalc: Program to generate domestic hot water profiles with statistical means for user defined conditions. (pp. 8-12). Orlando, USA: Proc. ISES Solar World Congress .

Kalogirou, S. (2004). Solar thermal collectors and applications. . *Elsevier , 30* (3), 231-295.

Klein, S., Cooper, P., Freeman, T., Beekman, D., Beckman, W., & Duffie, J. (1975). A method of simulation of solar processes and its application. *Solar Energy , 17*, 29-37.

KNMI. (2014, 3 1). *Klimatologie Daggegevens van het weer in Nederland - Download*. Retrieved 4 14, 2014 from Koninklijk Nederlands Meteorologisch Instituut : http://www.knmi.nl/klimatologie/daggegevens/selectie.cgi

Kumar, S., & Tiwar, G. (2009). Life cycle cost analysis of single slope hybrid (PV/T) active solar still. *Applied Energy , 86*, 1995–2004.

Nafey, A. (2005). Simulation of solar heating systems—an overview . *Renewable and Sustainable Energy Reviews* (9), 576–591 .

Newton, B. J. (1995). Master Thesis: Modeling of solar storage tanks. Wisconsin: University of Wisconsin.

Pachkawade, M., Nimkar, P., & Chavhan, B. (2013). Design and fabrication of low cost solar water heater. *International Journal of Emerging Trends in Engineering and Development , Vol. 6* (3).

PRC Bouwcentrum BV. (2004). *EPC en energieverbruik nieuwbouwwoningen .* Client: VROM/DGW. Utrecht, NL: VROM/DGW.

PV Magazine. (2014). *Module price index*. Retrieved May 15, 2014 from PV Magazine: http://www.pv-magazine.com/investors/module-price-index/#axzz32zoKGFgl

Rodríguez-Hidalgo, M. C., Rodríguez-Aumente , P., Lecuona, A., Legrand, M., & Ventas, R. (2012). Domestic hot water consumption vs. solar thermal energy storage: The optimum size of the storage tank. *Applied Energy , 97*, 897-906.

Sandnes, B., & Rekstad, J. (2002). A photovoltaic/thermal (PV/T) collector with a polymer absorber plate; Experimental study and analytical model. *Sol Energy , 72* (1), 63-73.

Santbergen, R., Rindt, C., Zondag, H., & van Zolingen, R. (2010). Detailed analysis of the energy yield of systems with covered sheet-and-tube PVT collectors. *Solar Energy , 84*, 867-878.

Sarhaddi, F., Farahat, S., Ajam, H., Behzadmehr, A., & Mahdavi Adeli , M. (2010). An improved thermal and electrical model for a solar photovoltaic thermal (PV/T) air collector. *Applied Energy* (87), 2328–2339 .

SER. (2013, September). *Energie Akkoord SER*. Retrieved May 20, 2014 from http://www.energieakkoordser.nl/~/media/9e6bae148edc4e67be1ae4f01723616e.ashx

SMZ. (2013). *Inventarisatie PV markt Nederland - Status oktober 2013 .* Stichting Monitoring Zonnestroom. Utrecht, NL: Zonnestroom.nl.

Tang, C. C. (2003). *Thesis: Modeling packaged heat pumps in a quasi-steady state energy simulation program .* Oklahoma State University.

TESS. (2013). (T. E. Specialists, Producer) Retrieved June 25, 2014 from TRNSYS - Features : http://www.trnsys.com/features/

Triple Solar. (2013). *Triple Solar - Installatie*. (Triple Solar) From Triple Solar: http://www.triplesolar.eu/ned/installatie.html

Twidell, A., & Weir, J. (2006). Renewable Energy Resources. London and New York: Taylor & Francis.

VFK. (2012, May -). *Vereniging van fabrikanten van ketels: De HR-ketel, een Nederlands feestje.* Retrieved June 26, 2014 from VFK: http://vfk.nl/wp-content/uploads/2012/06/1205VV-hr-ketel-een-nederlands-feestje.pdf

Zondag, H. (2008). Flat-plate PV-Thermal collectors and systems: A review . *Renewable and Sustainable Energy Reviews , 12*, 891-959.

Zondag, H., & van Helden, W. (2003). PV-T Thermal domestic systems. *3rd World Conference on Photovoltaic Energy Conversion.* Osaka, Japan: ECN.

Zondag, H., & van Helden, W. (2003). PV-thermal domestic systems. *3th World Conference on Photovoltaic Energy Conversion.* Osaka, Japan: ECN.

Zondag, H., & Van Helden, W. (2002). Stagnation temperature in PVT collectors. Rome.
Zondag, H., de Vries, D., van Helden, W., van Zolingen, R., & van Steenhoven, A. (2002). The thermal and electrical yield of a PV-thermal collector. *72, No. 2*, pp. 113-128. Solar Energy.

Zondag, H., de Vries, D., van Helden, W., van Zolingen, R., & van Steenhoven, A. (2003). The yield of different combined PV-thermal collector designs. *Solar Energy , 74*, 253-269.